2

HREC-0082-24
LMSC/HREC D162375

NTIS HC $4.75

LOCKHEED MISSILES & SPACE COMPANY
HUNTSVILLE RESEARCH & ENGINEERING CENTER
HUNTSVILLE RESEARCH PARK
4800 BRADFORD DRIVE, HUNTSVILLE, ALABAMA

CALCULATION OF STABILITY DERIVATIVES FOR SLOWLY OSCILLATING BODIES OF REVOLUTION AT MACH 1.0

February 1971

Contract NAS8-20082

Prepared for National Aeronautics and Space Administration
Marshall Space Flight Center, Alabama 35812

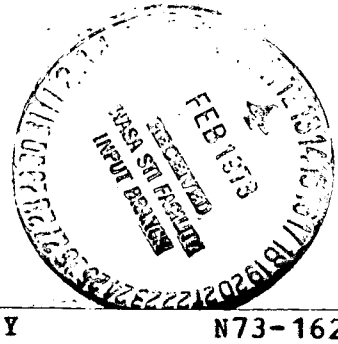

by
S. Y. Ruo
D. D. Liu

APPROVED: B. Hobson Shirley

B. Hobson Shirley, Supervisor
Aerophysics Section

George D. Reny

George D. Reny, Manager
Aeromechanics Department

FOREWORD

This report presents the results of work performed by Lockheed's Huntsville Research & Engineering Center while under subcontract to Northrop Nortronics (NSL PO 5-09287) for the Aero-Astrodynamics Laboratory of Marshall Space Flight Center, Contract NAS8-20082. This task was conducted in response to the requirement of Appendix B, Schedule Order 152, under the direction of Richard Beranek, Unsteady Aerodynamics Branch.

ACKNOWLEDGEMENTS

The authors are grateful to Dr. Max F. Platzer of the Research Laboratory, Lockheed-Georgia Company, for his constant encouragement, guidance and review of the manuscript, and to Mr. Robert A. Lott, Lockheed/Huntsville, for his constructive comments.

SUMMARY

Oswatitsch and Keune's parabolic method for steady transonic flow is applied and extended to bodies of revolution oscillating in a sonic flow field. A Laplace transform technique was employed to derive the dipole solution, and the Adams-Sears iterative technique was used in the stability derivative calculation.

A computer program was developed to perform the stability derivative calculation for the slowly oscillating cone and parabolic ogive. Inputs for the program are body geometry, thickness ratio, acceleration constant Γ and the pitch-axis location.

Sample calculations were performed for the parabolic ogive and circular cone. These results are compared with those obtained by using other techniques and the available experimental data for circular cones. For circular cones, the numerical studies show that the present results agree quite well with the available experimental static stability data and the calculated pitch-damping falls between Wehrend and Yanagizawa's experimental results. These comparisons show that the present analysis indicates a favorable trend. Finally, a possible method of improving the present analysis is proposed.

TABLE OF CONTENTS

APPENDIX

LIST OF FIGURES

NOMENCLATURE

A	$\Gamma + 2ik$, Eq. (2.10)
a	body pitch axis location
C_∞	freestream sound velocity
c	Euler's constant = 0.57721567
C_m	pitch moment coefficient = pitching moment/$q^*_\infty Q^* (\ell^*) \ell^*$
C_N	normal force coefficient = normal force/$q^*_\infty Q^* (\ell^*)$
$C_{N_\alpha}, C_{m_\alpha}$	stability derivatives due to angle of attack
$C_{N_{\dot\alpha}}, C_{N_q}$ $C_{m_{\dot\alpha}}, C_{m_q}$	stability derivatives due to total damping-in-pitch
$C_{N_\delta}, C_{m_\delta}$	in-phase flutter derivatives
$C_{N_{\dot\delta}}, C_{m_{\dot\delta}}$	out-of-phase flutter derivatives
C_p	pressure coefficient = $\left(P^* - P^*_\infty\right)/q^*_\infty$
C_{p_o}	pressure coefficient due to steady axial flow
C_{p_1}	in-phase pressure coefficient derivative = $\frac{1}{\cos\theta}\left(\frac{\partial C_p}{\partial \delta}\right)_{\delta \to 0}$
C_{p_2}	out-of-phase pressure coefficient derivative = $\frac{1}{\cos\theta}\left(\frac{\partial C_p}{\partial \dot\delta}\right)_{\dot\delta \to 0}$
dC_{N_α}/dx	local normal force coefficient slope
e, exp	exponential function
$F(x)$	doublet distribution function

i	$\sqrt{-1}$
$K_o(\lambda r)$	modified Bessel function of the second kind of zero order
k	reduced frequency = $\omega^* \ell^* / U_\infty^*$
ℓ	body length
L^{-1}	Laplace inversion transform operator
M_∞	freestream Mach number = U_∞^* / C_∞^*
O	"order of"
p	Laplace transform parameter
$Q(x)$	body cross-sectional area = $2\pi R^2(x)$
q_∞	freestream dynamic pressure
$R(x)$	body radius
t	time measure in a body-fixed reference frame = $t^* U_\infty^* / \ell^*$
U_∞	freestream speed
$W(x)$	body centerline motion function defined by Eq. (3.5)
x_s	sonic point location
x, r, θ	body-fixed cylindrical coordinates
x, y, z	Cartesian coordinates
Γ	acceleration constant, Eq. (2.7)
γ	ratio of specific heats, 1.4 for air
$\delta(t)$	instantaneous angle of pitch
δ_o	amplitude of angle of pitch
ϵ	body thickness ratio = $R_{max}/\ell = R(1)$
$\zeta(x, t; \Gamma)$	second order correction function, Eq. (2.18)
λ	crossflow out-of-phase perturbation potential
ξ	dipole coordinate

π	= 3.14159265
Φ	complete time-dependent perturbation potential, Eq. (2.2)
ϕ	axial-flow perturbation potential
φ	pulsating source potential, solution of Eq. (2.10)
$\hat{\varphi}$	complex perturbation potential, solution of Eq. (2.4)
$\tilde{\varphi}$	dipole solution in Laplace transform plane defined by Eq. (2.13)
χ	reduced complex perturbation potential defined by Eq. (3.2)
Ψ	crossflow in-phase perturbation potential

Subscripts and Superscripts

$( )', ( )'', \text{etc.}$	derivatives with respect to the independent variable
$( )_x, ( )_{xx}, \text{etc.}$	partial derivatives
$\dot{( )}$	derivative with respect to time
$( )^{(1)}$	first-order quantity
$( )^{(2)}$	second-order quantity
$( )^{(1)+(2)}$	first-order plus second-order quantity
$( )_R$	real part
$( )_I$	imaginary part
$( )^*$	physical quantity with proper dimension

Section 1
INTRODUCTION

The basic small perturbation equation governing transonic flow over slender bodies is well established. Due to its nonlinearity, however, analytical (closed form) solutions are obtained only in a few special cases. In 1955, Oswatitsch and Keune (Ref. 1) introduced an approximate solution (parabolic method) to steady sonic flow over the front part of a half-body of revolution by assuming a linear variation of the perturbation velocity in the mean flow direction ($\Phi_{xx} \sim$ constant) for linearization of the transonic equation. Maeder et al (Refs. 2, 3 and 4) extended this approach to the entire transonic Mach number range and applied the theory to full bodies of revolution as well as two-dimensional airfoils. Later Maeder and Thommen (Refs. 4 and 5) and Hosakawa (Refs. 6 and 7) improved Oswatitsch and Keune's parabolic method by introducing a correction function accounting for the nonlinearity. The parabolic method was then improved substantially by Spreiter and Alksne's Local Linearization method (Refs. 8 and 9), which yields excellent agreement with experimental results. Recently, the method of parametric differentiation by Rubbert (Ref. 10) and Rubbert and Landahl (Ref. 11) greatly advances the state of the art of the transonic flow problem. Unfortunately, this solution does not appear in a workable form and immediate application to the unsteady case is not obvious.

In the unsteady transonic flow, Landahl (Refs. 12 and 13) following the fundamental development of Lin et al (Ref. 14) linearized the unsteady flow equation by assuming high-frequency ($k >> \epsilon^{2/3}$ for planar flow and $k >> \epsilon^2 \ell n \epsilon$ for axisymmetric flow) oscillation and extensively explored the equations for various two and three dimensional shapes. Hsu and Ashley (Ref. 15) further studied the blunt-nose slender bodies performing lateral oscillation by extending the work of Landahl (Ref. 12).

Within the frame of unsteady linearized transonic flow Liu (Ref. 16) extended Platzer and Hoffman's (Ref. 17) quasi-slender body theory for supersonic flow by adopting a body-fixed coordinate system to treat the half-body of revolution oscillating at sufficiently high frequencies in a sonic flow field ($M_\infty = 1$).

In the recent work of Teipel (Ref. 18) and Liu (Ref. 19) they included the "nonlinear term"* of the unsteady perturbation potential equation in the analysis of airfoils (Ref. 18) and bodies of revolution (Ref. 19) oscillating in a sonic flow field by extending Oswatitsch and Keune's parabolic method (Ref. 1). Calculated results for a NACA 65 A 005 airfoil oscillating at both high and low frequencies have been presented by Teipel (Ref. 18). The results showed remarkable agreement with Nelson and Berman's experimental data (Ref. 20). For the oscillating bodies of revolution Liu (Ref. 19) obtained the approximate solutions for both high and low frequencies (valid in the range $0 \leq k < 1$) but no numerical results were presented.

The material presented in this report is a continuation of Liu's work (Ref. 19). Following his analysis, a brief description of the derivation is repeated in this report for the reader's convenience. Stability derivative calculations were performed for slowly oscillating parabolic ogives and circular cones in a sonic flow field by applying Adams-Sears' (Ref. 21) iterative procedure.

Assuming a constant Γ (see Eq. 2.7) for a particular body of revolution implies that the x-derivative of the perturbation velocity in the main flow direction (φ_x) is constant or, at least, changes very slowly. For a parabolic half-body of revolution this assumption is nearly correct but is not valid for

*The "nonlinear term" actually is the linear term with variant coefficients appearing in the unsteady perturbation potential equation (see Eq. (2.4)). They are called "nonlinear terms" here to signify that they are the coupling terms contributed by the nonlinear term in the steady transonic perturbation equation to the unsteady crossflow perturbation equation.

cones. In spite of this limitation, calculated results for the circular cone, in addition to the parabolic ogive, have been presented in this report (see Section 5) to show its qualitative trend.

Due to the lack of experimental data for the oscillating parabolic ogive, no comparison between the calculated and experimental results has been made. There are only very few test data available for oscillating cones (Refs. 22, 23 and 24). It is apparent that more experimental work in the field of unsteady aerodynamics is urgently needed.

In the subsequent sections, a body-fixed coordinate system (Fig. 1) is adopted and all the quantities are non-dimensional except those superscripted with an asterisk (*).

Section 2
APPROXIMATE SONIC EQUATIONS AND SOLUTIONS

The detailed derivation of an approximate solution to the unsteady "nonlinear" transonic perturbation potential equation has already been presented by Liu in Ref. 19. Here, only a brief description of the derivation is presented. It has been shown (e.g., Landahl (Ref. 12)) that the transonic small perturbation potential $\Phi(x, r, \theta, t)$ has to satisfy the following equation

$$(1 - M_\infty^2)\Phi_{xx} + \frac{1}{r}\Phi_r + \frac{1}{r^2}\Phi_{\theta\theta} + \Phi_{rr} - 2M_\infty^2\Phi_{xt} - M_\infty^2\Phi_{tt} = M_\infty^2(\gamma+1)\Phi_x\Phi_{xx} \quad (2.1)$$

Assuming the body performs simple harmonic motion, the complete perturbation potential can be written in the form,

$$\Phi(x, r, \theta, t) = \phi(x, r) + \hat{\varphi}(x, r, \theta)\, e^{ikt} \quad (2.2)$$

Letting $M_\infty = 1.0$ and substituting Eq. (2.2) into Eq. (2.1) yields the following equations:

$$O(1): \quad \phi_{rr} + \frac{1}{r}\phi_r = (\gamma+1)\phi_x\phi_{xx} \quad (2.3)$$

$$O(\delta_o): \quad \hat{\varphi}_{rr} + \frac{1}{r}\hat{\varphi}_r + \frac{1}{r^2}\hat{\varphi}_{\theta\theta} - (2ik\hat{\varphi}_x - k^2\hat{\varphi}) = (\gamma+1)\frac{\partial}{\partial x}(\phi_x\hat{\varphi}_x), \quad (2.4)$$

where the term $\hat{\varphi}_x\hat{\varphi}_{xx}\left(e^{ikt}\right)^2$ is neglected assuming small amplitude oscillations (Ref. 18).

The basic dipole solution $\hat{\varphi}$ can be obtained from the source solution φ by the following relation

$$\hat{\varphi} = \frac{\partial\varphi}{\partial r}\cos\theta \quad (2.5)$$

By substituting the above relation into Eq. (2.4), one obtains

$$\varphi_{rr} + \frac{1}{r}\varphi_r - 2ik\varphi_x + k^2\varphi = (\gamma+1)(\phi_x\varphi_{xx} + \phi_{xx}\varphi_x) . \tag{2.6}$$

Oswatitsch and Keune (Ref. 1) solved Eq. (2.3) by approximating

$$(\gamma+1)\phi_{xx} = \Gamma = \text{constant} > 0^{*} . \tag{2.7}$$

Equation (2.3) becomes

$$\phi_{rr} + \frac{1}{r}\phi_r = \Gamma\phi_x . \tag{2.8}$$

The parabolic solution of Eq. (2.8) has been given by Oswatitsch and Keune (Ref. 1) as

$$\phi(x,r) = -\frac{1}{4\pi}\int_0^x f(\xi)\cdot\exp\left[-\frac{\Gamma r^2}{4(x-\xi)}\right]\cdot\frac{d\xi}{x-\xi} . \tag{2.9}$$

Ignoring the term $(\gamma+1)\phi_x\varphi_{xx}$ in Eq. (2.6) and applying the relation in Eq. (2.7), one reduces Eq. (2.6) to

$$\varphi_{rr} + \frac{1}{r}\varphi_r - A\varphi_x + k^2\varphi = 0 \tag{2.10}$$

where $A = \Gamma + 2ik$.

Laplace transform in the x-direction transforms Eq. (2.10) into

$$\overline{\varphi}_{rr} + \frac{1}{r}\overline{\varphi}_r - \lambda^2\overline{\varphi} = 0 , \tag{2.11}$$

*For convenience, Γ is called the acceleration constant in the subsequent sections.

where

$$\lambda^2 = (\Gamma + 2ik)\, p - k^2$$

$$\overline{\varphi}(p, r) = \int_0^\infty \varphi(x, r)\, e^{-px}\, dx\ .$$

The solution of Eq. (2.11) is

$$\overline{\varphi}(p, r) = -\frac{1}{2\pi}\, \overline{F}(p)\, K_o(\lambda r) \tag{2.12}$$

where $K_o(\lambda r)$ is the modified Bessel function of the second kind of order zero.

The dipole solution then is

$$\widetilde{\varphi}(p, r, \theta) = \frac{\partial \overline{\varphi}}{\partial r} \cos\theta = -\frac{\cos\theta}{2\pi}\, \overline{F}(p)\, \frac{\partial}{\partial r} K_o(\lambda r) = \frac{\cos\theta}{2\pi}\, \lambda \overline{F}(p)\, K_1(\lambda r)\ . \tag{2.13}$$

Expanding $K_1(\lambda r)$ for small r and performing the inverse Laplace transform, one obtains the following dipole solution in the physical plane.

$$\begin{aligned}
\hat{\varphi}(x, r, \theta) &= \mathcal{L}^{-1}\left[\widetilde{\varphi}\right] \\
&= \frac{F(x)}{2\pi r} \cos\theta \\
&+ \frac{\Gamma r \cos\theta}{8\pi} \left\{ F'(x) \left[\ell n \frac{r^2}{2} + \eta(\Gamma, k) \right] - \int_0^x F''(\xi)\, \ell n(x - \xi)\, d\xi \right\} \\
&+ \frac{ikr\cos\theta}{4\pi} \left\{ F'(x) \left[\ell n \frac{r^2}{2} + \eta(\Gamma, k) \right] - \int_0^x F''(\xi)\, \ell n(x - \xi)\, d\xi \right\} \\
&- \frac{k^2 r \cos\theta}{8\pi} \left\{ F(x) \left[\ell n \frac{r^2}{2} + \eta(\Gamma, k) \right] - 2 \int_0^x F'(\xi)\, \ell n(x - \xi)\, d\xi \right. \\
&\left. + \int_0^x F''(\xi)\, (x - \xi)\, \ell n(x - \xi)\, d\xi \right\},
\end{aligned} \tag{2.14}$$

where

$$\eta(\Gamma, k) = \frac{1}{2}\ell n\left(k^2 + \frac{\Gamma^2}{4}\right) + c - 1 + i\left[\frac{\pi}{2} - \tan^{-1}\left(\frac{\Gamma}{2k}\right)\right] . \tag{2.15}$$

Equation (2.14) is the general parabolic dipole solution for Eq. (2.10). Since the present report is only concerned with the low frequency case, Eq. (2.14) can be further simplified by applying the following "low frequency" assumptions (Ref. 19), i.e.,

$$\begin{aligned} k &< 1 \\ k &= O[\Gamma]^* . \end{aligned} \tag{2.16}$$

Introducing the low frequency parameter $\mu = k/\Gamma < 1$ and requiring the quadratic and product terms of μ and k be negligible in the expression (2.14) gives

$$\hat{\varphi}(x, r, \theta) = \left[\frac{F(x)}{2\pi r} + \zeta(x, r; \Gamma)\right]\cos\theta \tag{2.17}$$

where

$$\begin{aligned} \zeta(x, r; \Gamma) = {} & \frac{\Gamma r}{8\pi}\left\{F'(x)\left(\ell n\frac{\Gamma r^2}{4} + c - 1\right) - \int_0^x F''(\xi)\,\ell n(x - \xi)\,d\xi\right\} \\ & + \frac{ikr}{4\pi}\left\{F'(x)\left(\ell n\frac{\Gamma r^2}{4} + c\right) - \int_0^x F''(\xi)\,\ell n(x - \xi)\,d\xi\right\} . \end{aligned} \tag{2.18}$$

It has been noted previously (Ref. 19) that the above low frequency solution is most suitable for applying the Adams-Sears iterative procedure (Ref. 21). Hence, the stability derivative calculation can yield a finite value for the limiting case of $k \to 0$.

*$k = O(\Gamma) \Rightarrow \lim_{\Gamma \to 0} k/\Gamma < \infty$: $0 < k < 1$

$k = O(\Gamma) \Rightarrow \lim_{\Gamma \to 0} k/\Gamma = 0$: $\mu < 1$

Section 3
BOUNDARY CONDITIONS AND ITERATIVE PROCEDURES

This section describes the application of the Adams and Sears iterative procedure (Ref. 21) to determine the dipole distribution F(x) in Eq. (2.17). The present report follows closely the procedure used in Ref. 16.

In addition to the boundary conditions at infinity the solution must also satisfy the tangency conditions at the body (Ref. 17):

$$\left.\begin{aligned} \phi_r &= R'(x)\cdot(1+\phi_x) \\ \Psi_r &= -1 + R'(x)\cdot\Psi_x \\ \lambda_r &= -\left[(x-a) + R(x)\cdot R'(x)\right] + R'(x)\cdot\lambda_x \end{aligned}\right\} \quad \text{at } r = R(x), \tag{3.1}$$

where

$\Psi(x,r)$: in-phase perturbation potential, and
$\lambda(x,r)$: out-of-phase perturbation potential.

The reduced potential $\chi(x,r)$ is defined as

$$\chi(x,r) = \frac{\hat{\phi}(x,r,\theta)}{\cos\theta} = \delta\,\Psi(x,r) + \dot{\delta}\,\lambda(x,r)\,. \tag{3.2}$$

From the relations in Eqs. (3.2) and (2.17), one can easily obtain the following relation

$$\chi(x,r) = \frac{F(x)}{2\pi r} + \zeta(x,r;\Gamma)\,. \tag{3.3}$$

By differentiating Eq. (3.2) with respect to r and utilizing the relations in Eq. (3.1), one gets

$$\chi_r\Big|_{r=R(x)} = -W(x) + R'(x) \cdot \chi_x \,, \tag{3.4}$$

where

W(x) is the body center-line motion function and expressed as

$$W(x)\Big|_{r=R(x)} = \delta + \left[(x-a) + \frac{Q'}{2\pi}\right] \dot{\delta} \,. \tag{3.5}$$

Applying the Adams-Sears' iteration procedure one can write

$$\chi(x,r) = \chi^{(1)} + \chi^{(2)} \tag{3.6}$$

and

$$F(x) = F^{(1)} + F^{(2)} \tag{3.7}$$

The first term on the right-hand side of Eqs. (3.6) and (3.7) is the slender body term and the second term represents the correction for the body thickness and the acceleration constant Γ^*. Substituting the above relations into Eq. (3.3) and collecting the terms of like order gives:

$$\chi^{(1)} = \frac{F^{(1)}}{2\pi r} \tag{3.8}$$

$$\chi^{(2)} = \frac{F^{(2)}}{2\pi r} + \zeta^{(1)}(x, r; \Gamma) \,. \tag{3.9}$$

From Eqs. (3.4), (3.8) and (3.9) one obtains the following relations:

$$\left.\begin{aligned} \frac{F^{(1)}(x)}{2\pi r^2} &= W^{(1)}(x) \\ -\frac{F^{(2)}(x)}{2\pi r^2} + \frac{\partial \zeta^{(1)}}{\partial r} &= -W^{(2)}(x) + R'(x) \cdot \chi_x^{(1)} \end{aligned}\right\} \quad \text{at } r = R, \tag{3.10}$$

*Γ is also thickness dependent, but this is related to the nonlinearity of the sonic flow.

where

$$\left.\begin{aligned} W^{(1)}(x) &= \delta + (x-a)\,\dot{\delta} \\ W^{(2)}(x) &= \frac{Q'(x)}{2\pi}\,\dot{\delta} \end{aligned}\right\}, \tag{3.11}$$

and

$$W(x) = W^{(1)}(x) + W^{(2)}(x)$$

By substituting the relations in Eq. (3.11) into Eq. (3.10) and after a simple rearrangement, one can write:

$$F^{(1)}(x) = 2Q(x)\left[\delta + (x-a)\dot{\delta}\right] \tag{3.12}$$

$$F^{(2)}(x) = \left[-\frac{Q'^2(x)}{\pi}\right]\delta + \left[-(x-a)\frac{Q'^2(x)}{\pi}\right]\dot{\delta} + 2Q(x)\frac{\partial \zeta^{(1)}}{\partial r} \tag{3.13}$$

Substituting Eq. (2.18) into Eq. (3.13), $F^{(2)}(x)$ becomes (see Appendix A for details):

$$F^{(2)}(x) = \delta\left[-\frac{Q'^2(x)}{\pi} + 2Z_R\,Q(x)\right] + \dot{\delta}\left[-(x-a)\frac{Q'^2(x)}{\pi} + 2Z_I\,Q(x)\right] \tag{3.14}$$

Upon comparing the relations in Eqs. (3.2) and (3.3) and utilizing the expressions for $F^{(1)}$ (Eq. 3.12), $F^{(2)}$ (Eq. 3.14) and $\zeta^{(1)}$ (Eq. A.2), one finally obtains the in-phase and out-of-phase cross flow potential valid to the second-order as:

$$\Psi^{(1)+(2)} = \frac{Q(x)}{\pi r}\left[1 + Z_R\right] - \frac{Q'^2(x)}{2\pi^2 r} + r\left[V_R \ln\frac{\Gamma r^2}{4} + Y_R\right] \tag{3.15}$$

$$\lambda^{(1)+(2)} = \frac{Q(x)}{\pi r}\left[(x-a) + Z_I\right] - (x-a)\frac{Q'^2(x)}{2\pi^2 r} + r\left[V_I \ln\frac{\Gamma r^2}{4} + Y_I\right], \tag{3.16}$$

where

$$V_R = \frac{\Gamma}{4\pi} Q'(x) ,$$

$$V_I = \frac{\Gamma}{4\pi} \left[(x-a) Q'(x) + Q(x) \right] + \frac{Q'(x)}{2\pi} ,$$

$$Y_R = \frac{\Gamma}{4\pi} \left[(c-1) Q'(x) - \int_o^x Q''(\xi) \ln(x-\xi) \, d\xi \right] , \tag{3.17}$$

$$Y_I = \frac{\Gamma}{4\pi} \left\{ (c-1) \left[(x-a) Q'(x) + Q(x) \right] - \int_o^x \left[(\xi-a) Q''(\xi) + 2Q'(\xi) \right] \ln(x-\xi) \, d\xi \right\}$$

$$+ \frac{1}{2\pi} \left\{ c Q'(x) - \int_o^x Q''(\xi) \ln(x-\xi) \, d\xi \right\} ,$$

$$Z_R = V_R \left[2 + \ln \frac{\Gamma r^2}{4} \right] + Y_R , \text{ and}$$

$$Z_I = V_I \left[2 + \ln \frac{\Gamma r^2}{4} \right] + Y_I .$$

Section 4
CALCULATION OF STABILITY DERIVATIVES

The technique of using the results obtained in the preceding sections for the calculation of the stability derivatives has been shown in Ref. 17 and also used in Ref. 16. Once the in-phase (Ψ) and the out-of-phase (λ) potentials are obtained the calculation of the stability derivatives is straightforward.

4.1 PRESSURE COEFFICIENT

The pressure coefficient may be expanded for small frequency and amplitude, just as the perturbation potential Φ was expanded. That is

$$C_p(x, R, \theta, t) = C_{p_o}(x, R) + \left[\delta C_{p_1}(x, R) + \dot{\delta} C_{p_2}(x, R)\right] \cos\theta \ , \qquad (4.1)$$

where

C_{p_o} : pressure coefficient due to steady axial flow,

C_{p_1} : pressure coefficient due to in-phase cross flow, and

C_{p_2} : pressure coefficient due to out-of-phase cross flow.

At $M_\infty = 1$, the in-phase and out-of-phase pressure coefficients evaluated on the body surface $r = R(x)$, valid to the second order, according to Platzer and Hoffman (Ref. 17) are

$$C_{p_1} = -2\,\Psi_x^{(1)+(2)} - R'^2(x) \cdot \Psi_x^{(1)}$$

$$C_{p_2} = -2\,(\lambda_x + \Psi)^{(1)+(2)} + 2\left[\Psi^{(1)} + R(x)\right]\phi_x^{(1)} - R'^2(x)\left[\lambda_x^{(1)} - \Psi^{(1)} - 2R(x)\right] , \qquad (4.2)$$

where

$$\Psi^{(1)}(x, r) = \frac{Q(x)}{\pi r} \text{ , and} \tag{4.3}$$

$$\lambda^{(1)}(x, r) = (x - a)\frac{Q(x)}{\pi r} . \tag{4.4}$$

The axial perturbation velocity on the body surface according to Spreiter and Alksne (Ref. 9):

$$\phi_x^{(1)}(x, R) = \frac{Q''(x)}{4\pi} \ell n \frac{\Gamma e^c Q(x)}{4\pi x} - \frac{1}{4\pi}\int_0^x \frac{Q''(\xi) - Q''(x)}{x - \xi} d\xi . \tag{4.5}$$

The local linearization method by Spreiter and Alksne (Ref. 9) further improved the cone-cylinder case by applying the sonic point condition at the shoulder. Thus, the improved solution for the cone may be used by letting $\ell/2 = 1$ in Eq. (64) of Ref. 9:

$$\phi_x(x, R) = \epsilon^2 \ell n\, \epsilon x - \frac{\epsilon^2}{2} \ell n \left\{ \epsilon^2 + \frac{4(1 - x^2)}{(\gamma+1)\epsilon^2 e^c} \right\} \tag{4.6}$$

Expressions of Ψ_x and λ_x are obtained by carrying out partial differentiation of the appropriate expressions of Ψ and λ with respect to x:

$$\begin{aligned}
\Psi_x^{(1)} &= \frac{Q'}{\pi R} \\
\Psi_x^{(1)+(2)} &= \frac{Q'}{\pi R}(1 + Z_R) + \frac{Q}{\pi R}\left(Z_R\right)_x - \frac{2Q'Q''}{2\pi^2 R} + R\left[\left(V_R\right)_x \ell n \frac{\Gamma R^2}{4} + \left(Y_R\right)_x\right] \\
\lambda_x^{(1)} &= \frac{Q}{\pi R} + (x - a)\frac{Q'}{\pi R} \\
\lambda_x^{(1)+(2)} &= \frac{Q'}{\pi R}\left[(x - a) + Z_I\right] + \frac{Q}{\pi R}\left[1 + \left(Z_I\right)_x\right] - (x - a)\frac{Q'Q''}{\pi^2 R} - \frac{Q'^2}{2\pi^2 R} \\
&\quad + R\left[\left(V_I\right)_x \ell n \frac{\Gamma R^2}{4} + \left(Y_I\right)_x\right],
\end{aligned} \tag{4.7}$$

where Z_R and Z_I are defined in Eq. (3.17), and

$$
\begin{aligned}
\left(V_R\right)_x &= \left(V_R\right)' = \frac{\Gamma}{4\pi}\,\Omega'' \\
\left(V_I\right)_x &= \left(V_I\right)' = \frac{\Gamma}{4\pi}\left[2\Omega' + (x-a)\Omega''\right] + \frac{\Omega''}{2\pi} \\
\left(Y_R\right)_x &= \left(Y_R\right)' = \frac{\Gamma}{4\pi}\left[(c-1)\Omega'' - I_4\right] \\
\left(Y_I\right)_x &= \left(Y_I\right)' = \frac{\Gamma}{4\pi}\left\{(c-1)\left[\Omega' + \Omega'' + (x-a)\Omega'''\right] - 3I_2 + aI_4 - I_5\right\} \\
&\qquad + \frac{1}{2\pi}\left\{c\Omega'' - I_2\right\} \\
\left(Z_R\right)_x &= \left(Z_R\right)' = \frac{\Gamma}{4\pi}\left[\Omega''\left(\ell n\frac{\Gamma\Omega}{4\pi} + c + 1\right) + \frac{\Omega'^2}{\Omega} - I_4\right] \\
\left(Z_I\right)_x &= \left(Z_I\right)' = \frac{\Gamma}{4\pi}\left\{\left[(x-a)\Omega'' + 2\Omega'\right]\left[\ell n\frac{\Gamma\Omega}{4\pi} + c + 1\right] + (x-a)\frac{\Omega'^2}{\Omega} + \Omega'\right. \\
&\qquad \left. - 3I_2 + aI_4 - I_5\right\} + \frac{1}{2\pi}\left\{\left[\ell n\frac{\Gamma\Omega}{4\pi} + c + 2\right]\Omega'' + \frac{\Omega'^2}{\Omega} - I_4\right\}.
\end{aligned}
\tag{4.8}
$$

Where I_2, I_4 and I_5 are defined as follows: (See Appendix C)

$$
\left.
\begin{aligned}
I_2 &= \int_0^x \Omega''(\xi)\,\ell n(x-\xi)\,d\xi \\
I_4 &= \int_0^x \Omega'''(\xi)\,\ell n(x-\xi)\,d\xi \\
I_5 &= \int_0^x \xi\,\Omega'''(\xi)\,\ell n(x-\xi)\,d\xi
\end{aligned}
\right\}. \tag{4.9}
$$

4.2 STABILITY DERIVATIVES

The four flutter derivatives are defined as (Ref. 17):

$$C_{N_\delta} = \left(\frac{\partial C_N}{\partial \delta}\right)_{\delta \to 0} = -\frac{\pi}{Q(l)} \int_o^l R\, C_{p_1}\, dx \tag{4.10}$$

$$C_{m_\delta} = \left(\frac{\partial C_m}{\partial \delta}\right)_{\delta \to 0} = \frac{\pi}{Q(l)} \int_o^l (x-a)\, R\, C_{p_1}\, dx + \frac{\pi}{Q(l)} \int_o^l R^2 R' C_{p_1}\, dx \tag{4.11}$$

$$C_{N_{\dot\delta}} = \left(\frac{\partial C_N}{\partial \dot\delta}\right)_{\dot\delta \to 0} = -\frac{\pi}{Q(l)} \int_o^l R\, C_{p_2}\, dx \tag{4.12}$$

$$C_{m_{\dot\delta}} = \left(\frac{\partial C_m}{\partial \dot\delta}\right)_{\dot\delta \to 0} = \frac{\pi}{Q(l)} \int_o^l (x-a)\, R\, C_{p_2}\, dx + \frac{\pi}{Q(l)} \int_o^l R^2 R' C_{p_2}\, dx \tag{4.13}$$

and related to stability derivatives by (Ref. 25):

$$\left.\begin{aligned} C_{N_\alpha} &= C_{N_\delta} \\ C_{m_\alpha} &= C_{m_\delta} \\ C_{N_{\dot\alpha}} + C_{N_q} &= C_{N_{\dot\delta}} \\ C_{m_{\dot\alpha}} + C_{m_q} &= C_{m_{\dot\delta}} \end{aligned}\right\} \tag{4.14}$$

In order to be consistent with the slender body assumption, only the terms up to second order in ϵ are considered in the force and moment coefficients. Hence, the last term on the right-hand side of Eqs. (4.11) and (4.13) is further simplified in the actual calculation. These two equations may be rewritten as

$$C_{m_\delta} = \frac{\pi}{Q(1)}\left[\int_0^1 (x-a)\,R\,C_{p_1}\,dx + \int_0^1 R^2\,R'\,C_{p_3}\,dx\right] \tag{4.15}$$

$$C_{m_{\dot\delta}} = \frac{\pi}{Q(1)}\left[\int_0^1 (x-a)\,R\,C_{p_2}\,dx + \int_0^1 R^2\,R'\,C_{p_4}\,dx\right], \tag{4.16}$$

where

$$C_{p_3} = -2\,\Psi_x^{(1)}$$

$$C_{p_4} = -2\left(\lambda_x^{(1)} + \Psi^{(1)}\right).$$

The expressions of C_{p_3} and C_{p_4} used in this study for a body of revolution with a radius of $R(x) = \epsilon Z(x)$ are given in Appendix B, Eqs. (B.6) and (B.7).

4.3 CALCULATION PROCEDURE

To calculate the stability derivatives for a certain pointed body of revolution, the integration may be carried out according to Eqs. (4.10) to (4.13) either analytically or numerically. In this report the numerical method is chosen in order to develop a more general computer program which can handle the various body shapes that are involved.

To carry out the integration numerically, however, one needs to evaluate the values of the integrand along x coordinate first. To calculate the local values of C_{p_1} and C_{p_2} on the body, one first must carry out the integrations that appeared in Eqs. (A.4), (A.6) and (4.8). These are integrated analytically as shown in Appendix C.

4.4 EVALUATION OF Γ

To carry out the calculation of the stability derivatives according to those equations obtained in the preceding articles, the value of the acceleration constant Γ must be first provided. The methods employed in this report are as follows:

- Circular Cone:

Based on the assumption Eq. (2.7) and the small perturbation velocity for the cone, Eq. (4.6), the following relation can be obtained:

$$\Gamma = \epsilon^2 (\gamma+1) \left[\frac{1}{x} + \frac{4x}{(\gamma+1)\,\epsilon^4\, e^c + 4(1-x^2)} \right] . \tag{4.17}$$

The value of Γ evaluated at $x = 1/2$ for cones of different thickness is plotted as curve (1) in Fig. 2.

- Parabolic Ogive

Maeder and Thommen (Ref. 4) and Hosokawa (Ref. 6) introduced a method to solve for the sonic point on the body and the Γ value by using the following relations

$$\left.\begin{aligned} \phi_x(x_s) &= 0 \\ \phi_{xx}(x_s) &= \frac{\Gamma}{\gamma+1} \end{aligned}\right\} . \tag{4.18}$$

In Fig. 2, curve (2) is given by Maeder and Thommen (Fig. 9 of Ref. 4) for the parabolic bodies of revolution, curve (3) is calculated according to conditions in Eq. (4.18) for the parabolic ogive with the flow potential given by Hosokawa (Ref. 6), curve (4) is calculated according to the following relation (letting $\ell = 2$ in Eq. (50) of Ref. 9):

$$\Gamma = 2(\gamma+1)\,\pi\,\epsilon^2 \tag{4.19}$$

Curve (2) in Fig. 2 given by Maeder and Thommen was originally calculated for the steady full parabolic body of revolution at Mach one. This value of Γ is used directly for the half parabolic body of revolution in this report. Since the physical condition along a parabolic ogive is the same as that along the forebody of the parabolic spindle of the same physical thickness, the sonic point will occur at the same point on both bodies. From Eq. (4.18) one can easily see that the same Γ value can be obtained for both parabolic ogive and parabolic spindle of the same thickness.

Section 5
NUMERICAL RESULTS AND DISCUSSIONS

5.1 APPLICATION TO BASIC BODY CONFIGURATIONS

To illustrate the effect of body geometry, thickness ratio, pitch axis location and the "nonlinear" contribution, i.e., terms associated with Γ on the static and dynamic stability derivatives, numerical examples were calculated for two basic configurations. They are:

1. Right Circular Cone $R(x) = \epsilon x$
2. Parabolic Ogive $R(x) = \epsilon x(2 - x)$.

Most of the numerical studies were compared with the previous linearized flow results (Ref. 16) and other available theoretical and experimental results (Refs. 12, 23 and 24).

5.2 DISCUSSION OF RESULTS

Stability derivatives were computed and plotted versus three parameters: body thickness, pitch axis location and the reduced frequency. In this present low frequency calculation, the acceleration constant Γ has to be preselected before the stability derivative calculation. The Γ values are based essentially on three previous steady transonic flow theories, i.e., Maeder-Thommen's theory (Ref. 4), Spreiter-Alksne's theory (Ref. 9) and Hosokawa's theory (Ref. 6). In Fig. 2, the acceleration constant Γ is plotted as a function of thickness ratio for the cone and ogive according to the different formulas provided by these theories.

The local normal force slope dC_{N_α}/dx for the cone and the parabolic ogive are shown in Figs. 3 through 5. In Figs. 4 and 5, the results calculated

for the ogive using the Γ value according to Maeder-Thommen and Spreiter-Alksne are presented. Since the Γ values are approximately equal, the results obtained using curve (3) (Hosokawa) are not very different from those obtained using curve (2) and these results (Hosokawa) are not presented in Figs. 4 and 5.

In Fig. 6, the normal force coefficients C_{N_α} based on different Γ values are plotted against body thickness ratio for a parabolic ogive. Large distinction and different trends of the thickness dependence are found for C_{N_α} when compared with the slender body and the previous linearized flow results. Good agreement with experimental results (Ref. 23) for a 12.5-degree cone is found in Figs. 7 and 8. In fact, the present calculation predicts, in general, closer results to experiment for both C_{N_α} and C_{m_α} than the linearized flow results. This result justifies that the present analysis is a more consistent one. In Fig. 9, the damping-in-pitch normal force coefficient $C_{N_{\dot\delta}}$ for a 10-degree cone is given in contrast to the various oscillating supersonic cone theories (Refs. 26, 27 and 28).

The damping-in-pitch moment coefficients $C_{m_{\dot\delta}}$ are given in Figs. 10 through 16. Figures 10 through 12 illustrate the pitch-axis location effect on $C_{m_{\dot\delta}}$ for a cone and an ogive. When compared with experimental results for a 12.5-degree cone (Fig. 11), the present results fall in between Wehrend's (Ref. 23) and Yanagizawa's (interpolated between 10-degree and 15-degree cones, Ref. 24) results. Figures 13 and 14 compare the thickness effect for a cone and an ogive with various pitch-axis location predicted by the present method, linearized flow theory (Ref. 16) and Landahl's theory (Ref. 13). It is seen that the slender body theory, in general, predicts a higher cone pitch-damping than the other theories.

Figure 15 presents the frequency dependence of damping-in-pitch moment coefficient $C_{m_{\dot\delta}}$ for parabolic ogives of different thickness. Previous linearized

flow and Landahl's results are also plotted for comparison. Note the invalidity of the linearized and Landahl's theory when the reduced frequency k approaches zero. In Fig. 16, the influence of body shape on the damping-in-pitch moment coefficient is demonstrated for a cone and an ogive of 0.1 thickness ratio. In contrast to the linearized theory, the present method indeed predicts a finite value as the reduced frequency k approaches zero.

Section 6
CONCLUDING REMARKS AND RECOMMENDATIONS

6.1 CONCLUDING REMARKS

In the preceding sections, the low frequency potential solution based on Oswatitsch-Maeder's linearization concept is applied and extended for calculating the aerodynamic forces and moments acting upon half bodies of revolution performing slow pitching harmonic oscillations. Using this solution, the present analysis can provide a finite value for the stability derivatives as the reduced frequency approaches zero. This value is of engineering interest and cannot be obtained through the previous linearization formulation (Refs. 13 and 16).

Following the previous work (Refs. 16 and 17), the Adams-Sears' iterative procedure was used to obtain the in-phase and out-of-phase perturbation potentials, thus facilitating calculation of the stability derivatives. The numerical studies showed that the present results agree quite well with the experimental value of static stability derivatives for the circular cone (Figs. 7 and 8). Comparison with the experimental results (Refs. 23 and 24) for the damping-in-pitch moment coefficient for the cone also shows that the present analysis indicates a favorable trend. These comparisons seem to substantiate the approximation made in the present analysis. However, to obtain the low frequency solution, it was necessary to approximate the governing equation (2.6), by ignoring the term $\phi_x \varphi_{xx}$; thus the approach cannot be completely justified mathematically. It is, therefore, essential to determine the error incurred in the present approximation and to further investigate new results based on some other improved solutions for comparison. No definite assessment of the technique described in this report can be made based on the currently available few test data for circular cones, though it shows a favorable trend.

In this study, the technique of selecting the acceleration constant, Γ, has been based on some analytical and semi-analytical methods. If the experimental data are available, however, the Γ value can be calculated from either the static or the dynamic test data. The validity of the method described in this report can also be checked by calculating the Γ value from the static data and using this Γ value to obtain the dynamic data. This calculated dynamic data is then compared against the dynamic test data.

6.2 RECOMMENDATIONS

Among the unsteady transonic flow studies, Hosokawa's (Refs. 6 and 7) nonlinear correction theory seems to offer immediate applicability for the present problem. His nonlinear correction procedure can account for the transonic nonlinearity, the effect of the transonic normal shock and, in the case of unsteady flow, the recovery of the term $\phi_x \varphi_{xx}$. By properly incorporating the nonlinear correction procedure to the present low frequency solution, one can obtain the "correction value" for the in-phase and out-of-phase potential, hence the "correction value" for the stability derivatives. This approach is now being pursued, and numerical studies will be performed for a parabolic ogive and a parabolic spindle, so that the error incurred due to the term $\phi_x \varphi_{xx}$ can be investigated from the results of parabolic ogive and the shock effect can be investigated from the parabolic spindle calculation.

Due to the lack of experimental data the evaluation of the present method is only partially successful. Therefore, it is strongly recommended that systematic, both static and dynamic, experiments on the body of revolution in the transonic flow range be performed to aid the advancement of the state of the art in this particular field of study.

REFERENCES

1. Oswatitsch, K., and F. Keune, "Flow Around Bodies of Revolution at Mach Number One," Proceedings of the Conference on High-Speed Aeronautics, Polytechnic Institute of Brooklyn, 20 - 22 January 1955.

2. Maeder, P.F., and H.U. Thommen, "Some Results of Linearized Transonic Flow about Slender Airfoils and Bodies of Revolution," J. Aero. Sci., Vol.23, No.2, 1956, pp.187-188.

3. Maeder, P.F., and A.D. Wood, "Linearized Transonic Flow past Isolated Non-Lifting Airfoils," Brown University, Division of Engineering, Technical Report WT-24, June 1957.

4. Maeder, P.F., and H.U. Thommen, "Linearized Transonic Flow About Slender Bodies of Revolution at Zero Incidence," Brown University, Division of Engineering, Technical Report WT-25, July 1957.

5. Maeder, P.F., and H.U. Thommen, "Linearized Transonic Flow About Slender Bodies at Zero Angle of Attack," Brown University, Division of Engineering, Technical Report WT-34, October 1960.

6. Hosokawa, I., "A Refinement of the Linearized Transonic Flow Theory," J. Phys. Soc. Japan, Vol.15, No.11, 1960, pp.149-157.

7. Hosokawa, I., "A Simplified Analysis for Transonic Flows Around Thin Bodies," IUTAM, Symposium Transsonicum, Aachen, 3-7 September 1962, Edited by Klaus Oswatitsch, Springer-Verlag, 1964, pp.184-199.

8. Spreiter, J.R., and A.Y. Alksne, "Thin Airfoil Theory Based on Approximate Solution of the Transonic Flow Equation," NACA Report 1359, 1958.

9. Spreiter, J.R., and A.Y. Alksne, "Slender-Body Theory Based on Approximate Solution of the Transonic Flow Equation," NASA TR R-2, 1959.

10. Rubbert, P.E., "Analysis of Transonic Flow by Means of Parametric Differentiation," AFOSR 65-1932, MIT Fluid Dynamics Research Laboratory Report 65-2, November 1965.

11. Rubbert, P.E., and M.T. Landahl, "Solution of the Transonic Airfoil Problem Through Parametric Differentiation," AIAA J., Vol.5, No.3, 1967, pp.470-479.

12. Landahl, M.T., "Forces and Moments on Oscillating Slender Wing-Body Combination at Sonic Speed," OSR Technical Note 56-109, February 1956.

13. Landahl, M.T., "Linearized Theory for Unsteady Transonic Flow," MIT Fluid Dynamics Research Laboratory Report No.63-2, March 1963.

14. Lin, C.C., E. Reissner and H.S. Tsien, "On Two-Dimensional Non-Steady Motion of a Slender Body in a Compressible Fluid," J. Math. Phy., Vol. XXVII, 1948, pp.220-231.

15. Hsu, P.T., and H. Ashley, "Introductory Study of Airloads on Blunt Bodies Performing Lateral Oscillations," MIT Fluid Dynamics Research Laboratory Report No.59-9, 1959.

16. Liu, D.D., "Quasi-Slender Body Theory for Unsteady Linearized Transonic Flow past Pointed Bodies of Revolution," LMSC/HREC A791435, Lockheed Missiles & Space Company, Huntsville, Ala., April 1968.

17. Platzer, M.F., and G.H. Hoffman, "Quasi-Slender Body Theory for Slowly Oscillating Bodies of Revolution in Supersonic Flow," NASA TN D-3440, June 1966.

18. Teipel, I., "Die Instationären Luftkräfte bei der Machzahl 1," Z. Flugwiss., 12, Heft 1 (1964): Also "The Nonsteady Aerodynamic Forces at Mach Number One," Translation, RSIC-808, Redstone Arsenal, Ala.

19. Liu, D.D., "Some Approximate Solutions for Oscillating Bodies of Revolution in Nonlinear Transonic Flow," Lockheed Missiles & Space Company, Huntsville, Ala., LMSC/HREC A791499, June 1968.

20. Nelson, H.C., and J.H. Berman, "Calculation of the Forces and Moments for an Oscillating Wing-Aileron Combination in Two-Dimensional Potential Flow at Sonic Speed," NACA Report 1128 (1953).

21. Adams, M.C., and W.R. Sears, "Slender-Body Theory-Review and Extension," J. Aero. Sci., Vol.20, No.2, 1953, pp.85-98.

22. Foster, A.D., "A Compilation of Longitudinal Aerodynamic Characteristics Including Pressure Information for Sharp- and Blunt-Nose Cones Having Flat and Modified Bases," Sandia Corporation Monograph SC-R-64-1311, January 1965.

23. Wehrend, W., Jr., "An Experimental Evaluation of Aerodynamic Damping Moments of Cones with Different Center of Rotation," NASA TN D-1768, March 1963.

24. Yanagizawa, M., "Measurement of Dynamic Stability Derivatives of Cones and Delta-Wings at High Speed," National Aeronautical Laboratory TR-172, Tokyo, Japan, 1969.

25. Van Dyke, M.D., "Supersonic Flow past Oscillating Airfoils Including Nonlinear Thickness Effects," NACA Report 1183 (1954).

26. Brong, E.A., "The Flow Field About a Right Circular Cone in Unsteady Flight," AIAA Paper No.65-398, presented at AIAA Second Annual Meeting, San Francisco, 26-29 July 1965.

27. Hsu, P.T., "Solution of the Supersonic Flow Field Around an Oscillating Circular Cone," MIT Fluid Dynamics Research Laboratory Report No.64-5, December 1964.

28. Tobak, M., and W.R. Wehrend, "Stability Derivatives of Cones at Supersonic Speeds," NACA TN 3788 (1956).

FIGURES

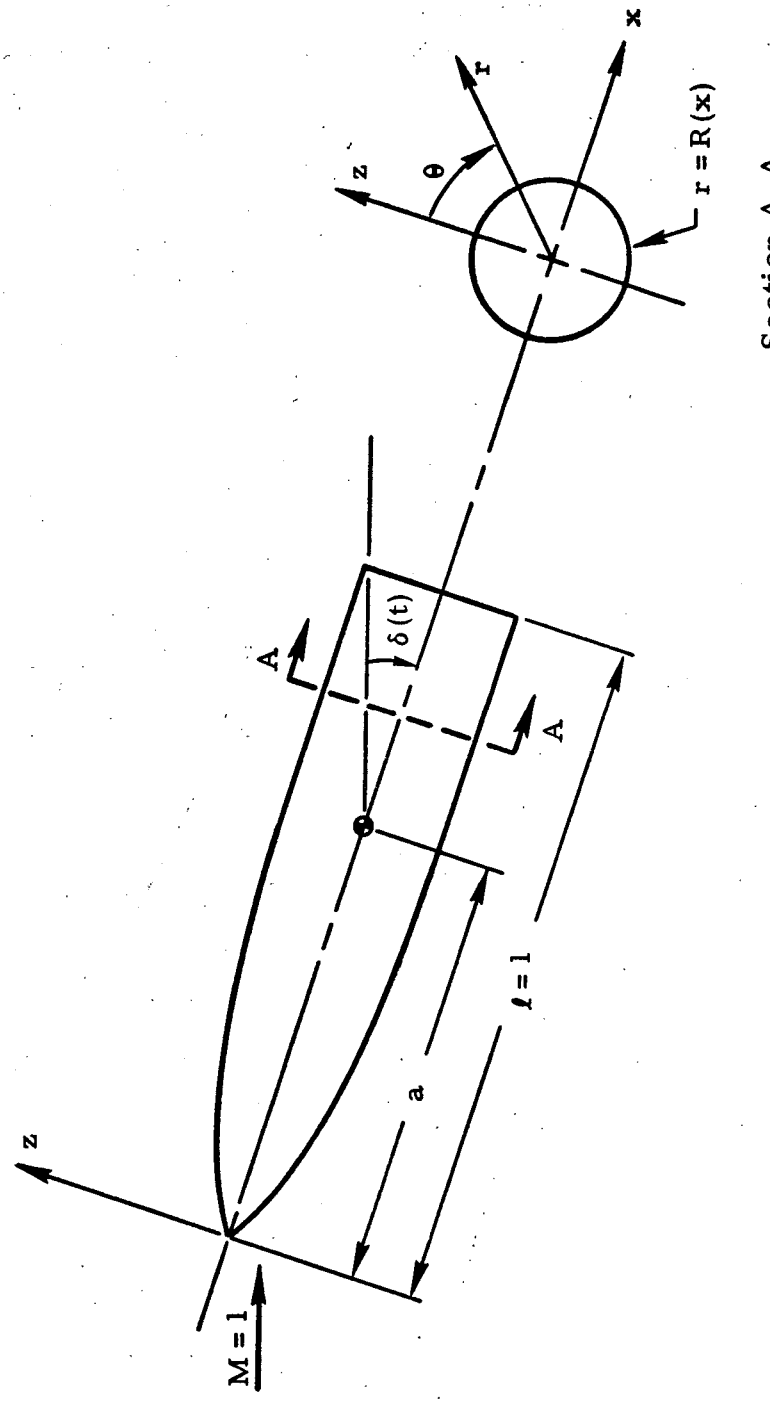

Fig. 1 - Body-Fixed Coordinate System

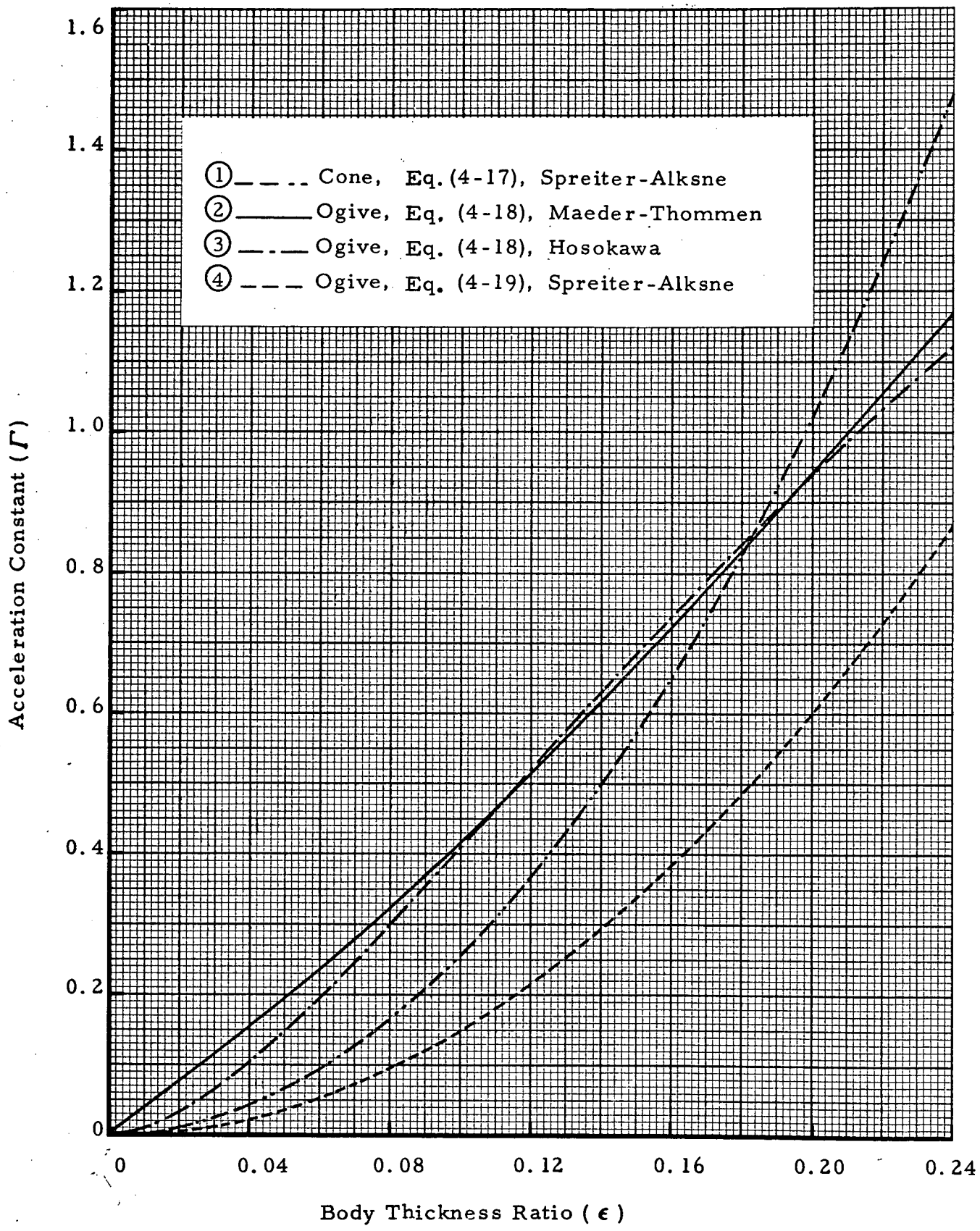

Fig. 2 - Acceleration Constant for Bodies of Different Thickness.

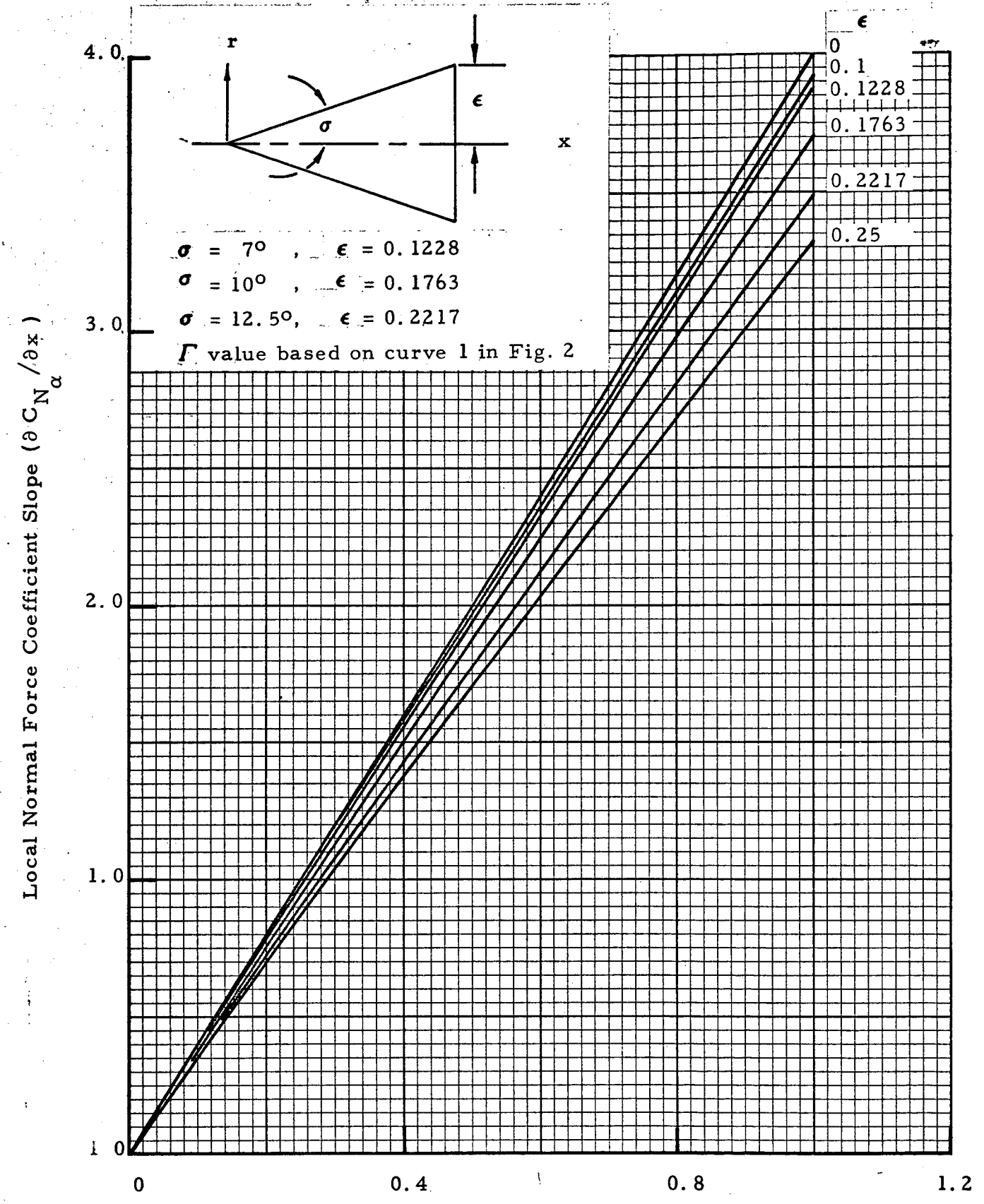

Fig. 3 - Local Normal Force Slope Variation for Cones at $M_\infty \neq 1.0$.

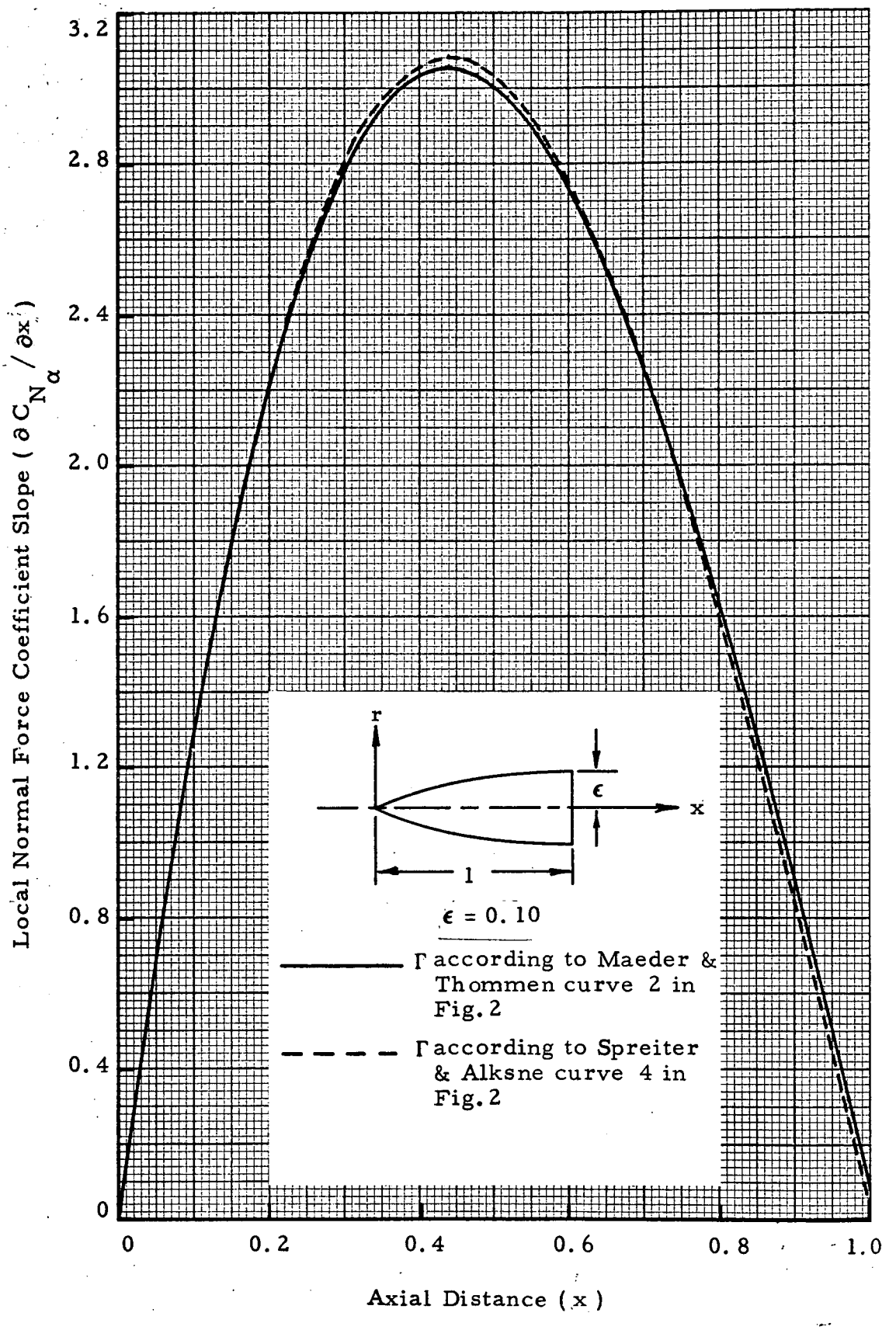

Fig. 4 - Local Normal Force Slope Variation for Parabolic Ogive of ϵ = 0.1 at M_∞ = 1.0

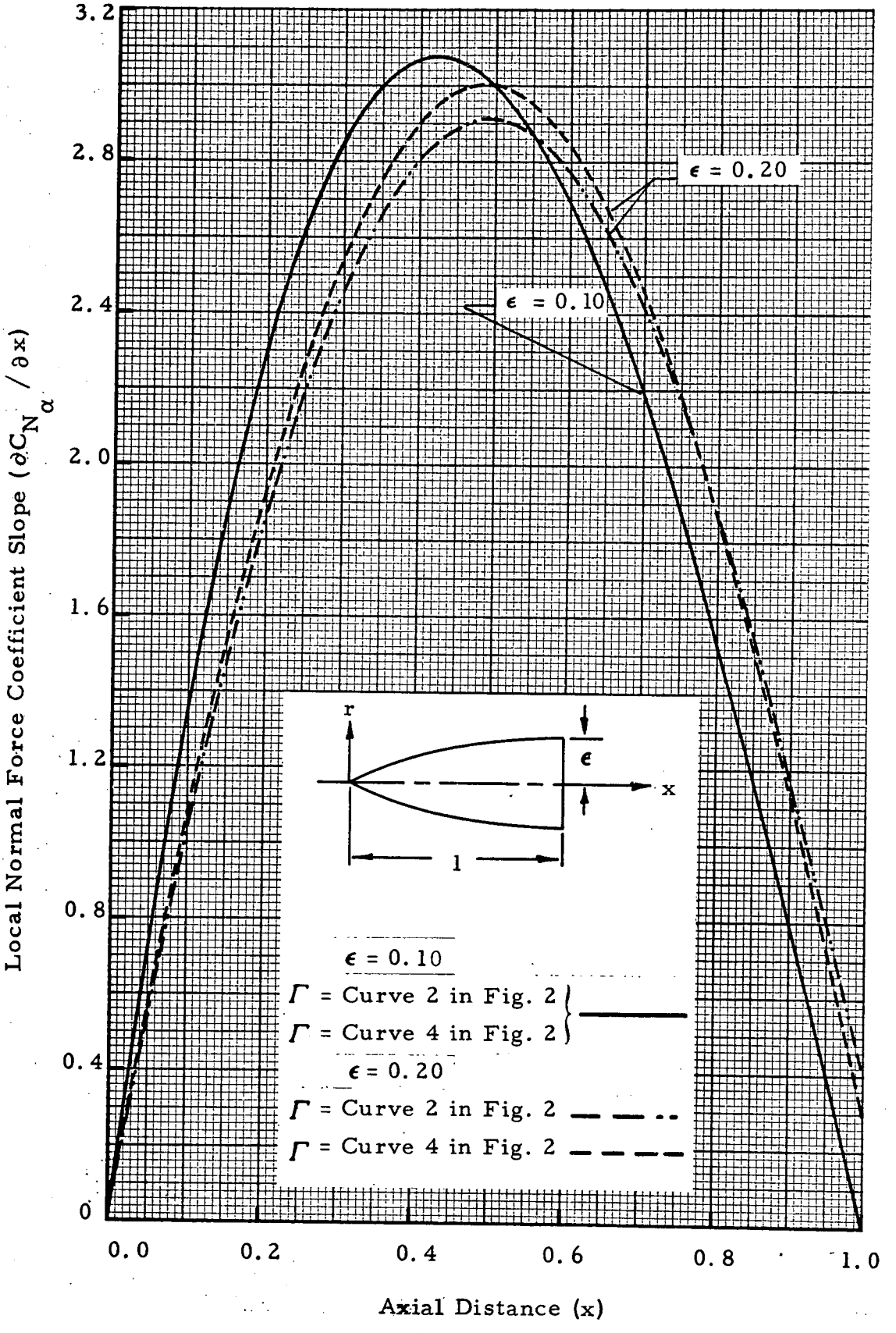

Fig. 5 - Local Normal Force Slope Variation for Parabolic Ogives at M_∞ = 1.0

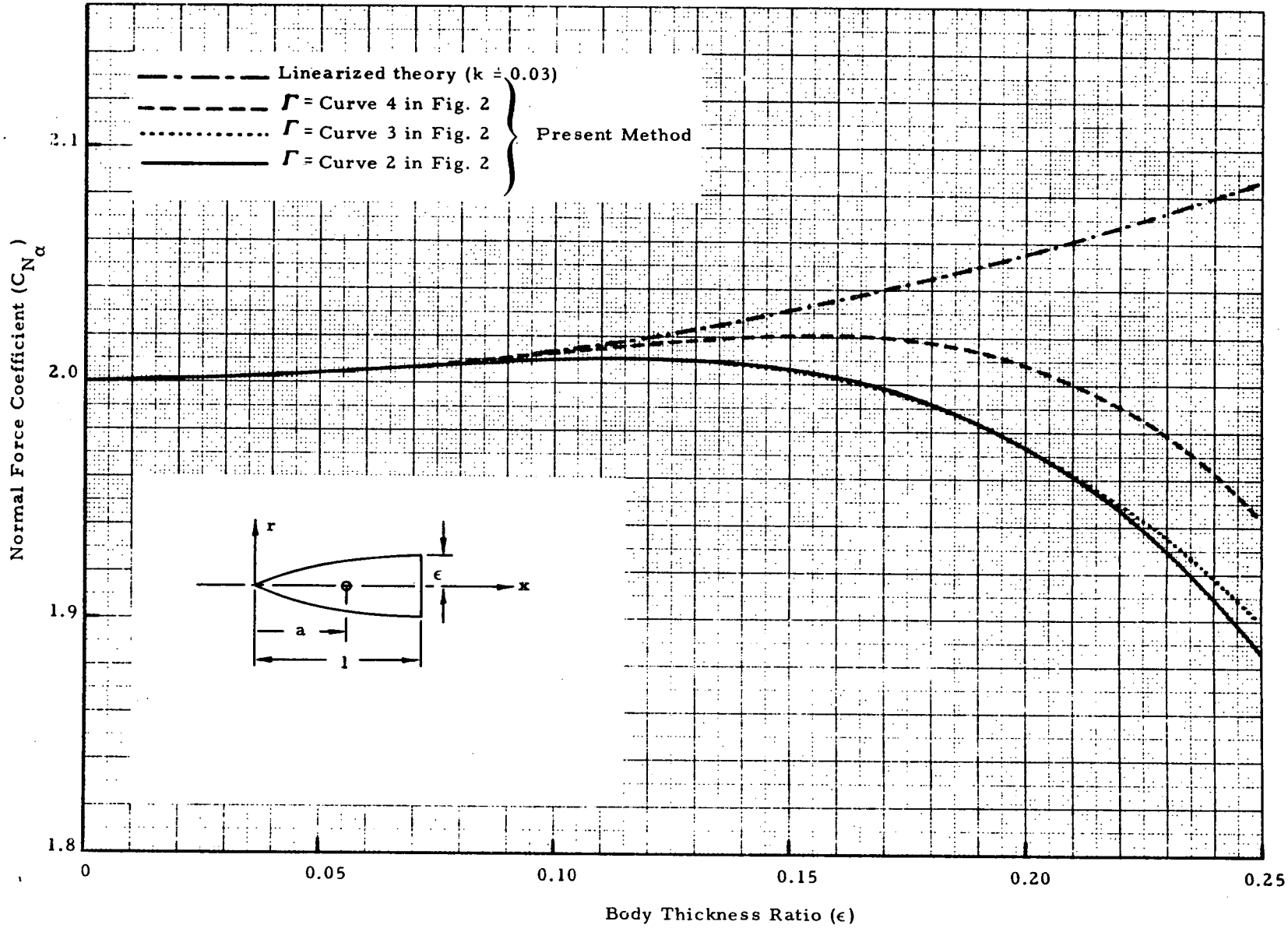

Fig. 6 - Effect of Thickness Ratio on Normal Force Coefficient for Parabolic Ogive at M_∞ = 1.0.

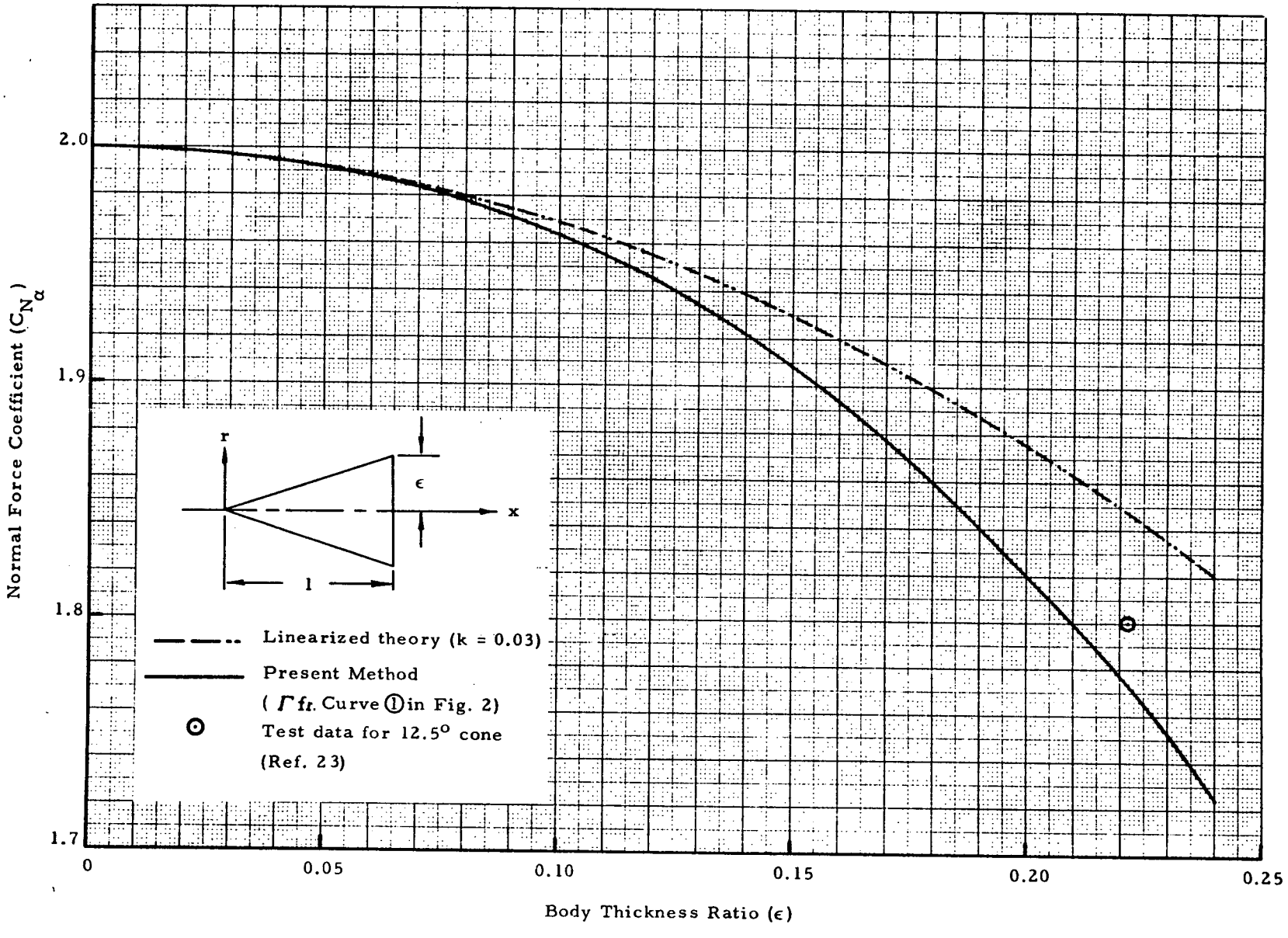

Fig. 7 - Effect of Thickness Ratio on Normal Force Coefficient for Circular Cone at M_∞ = 1.0.

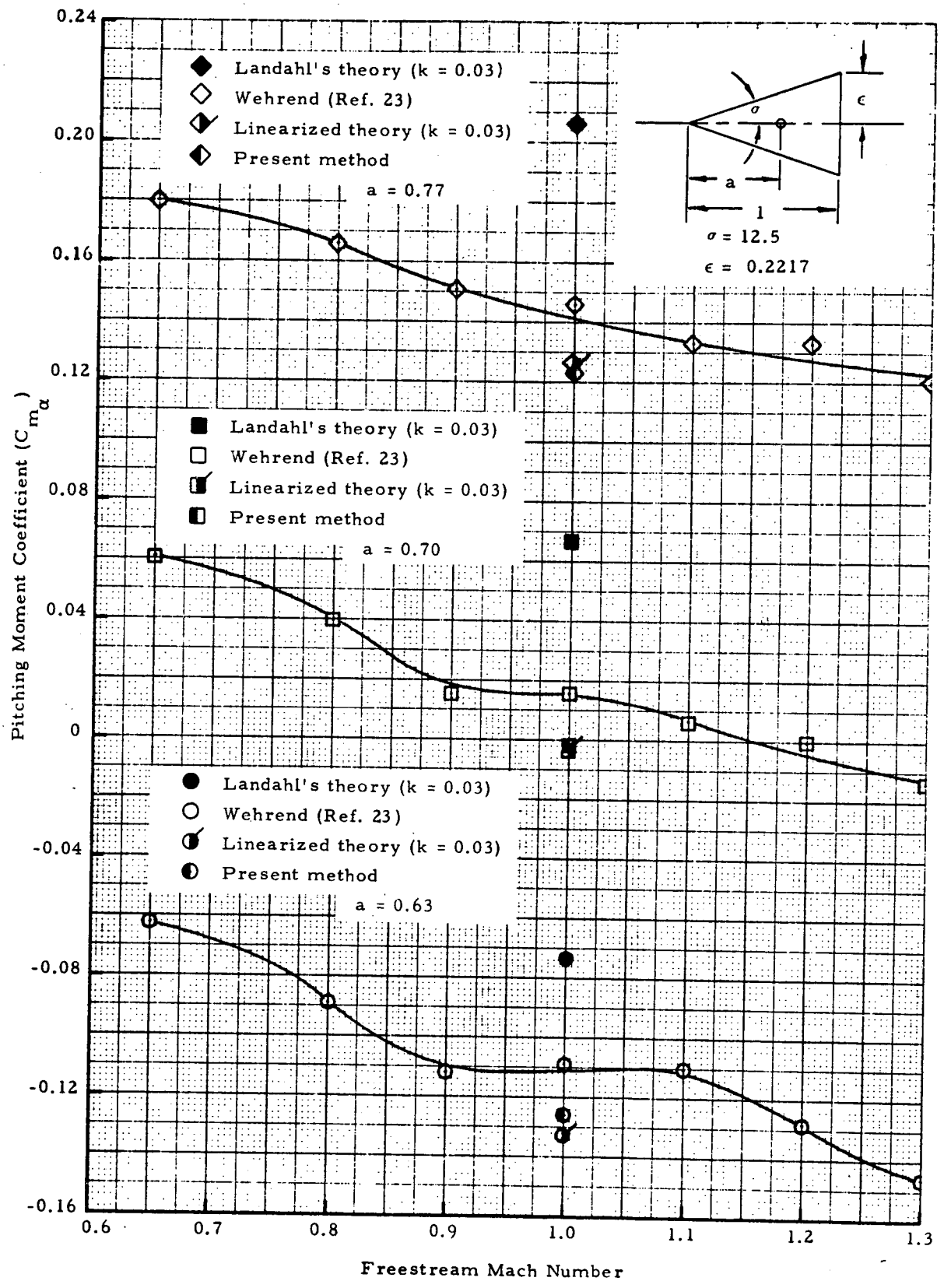

Fig. 8 - Pitching Moment Coefficient for a 12.5-Degree Cone.

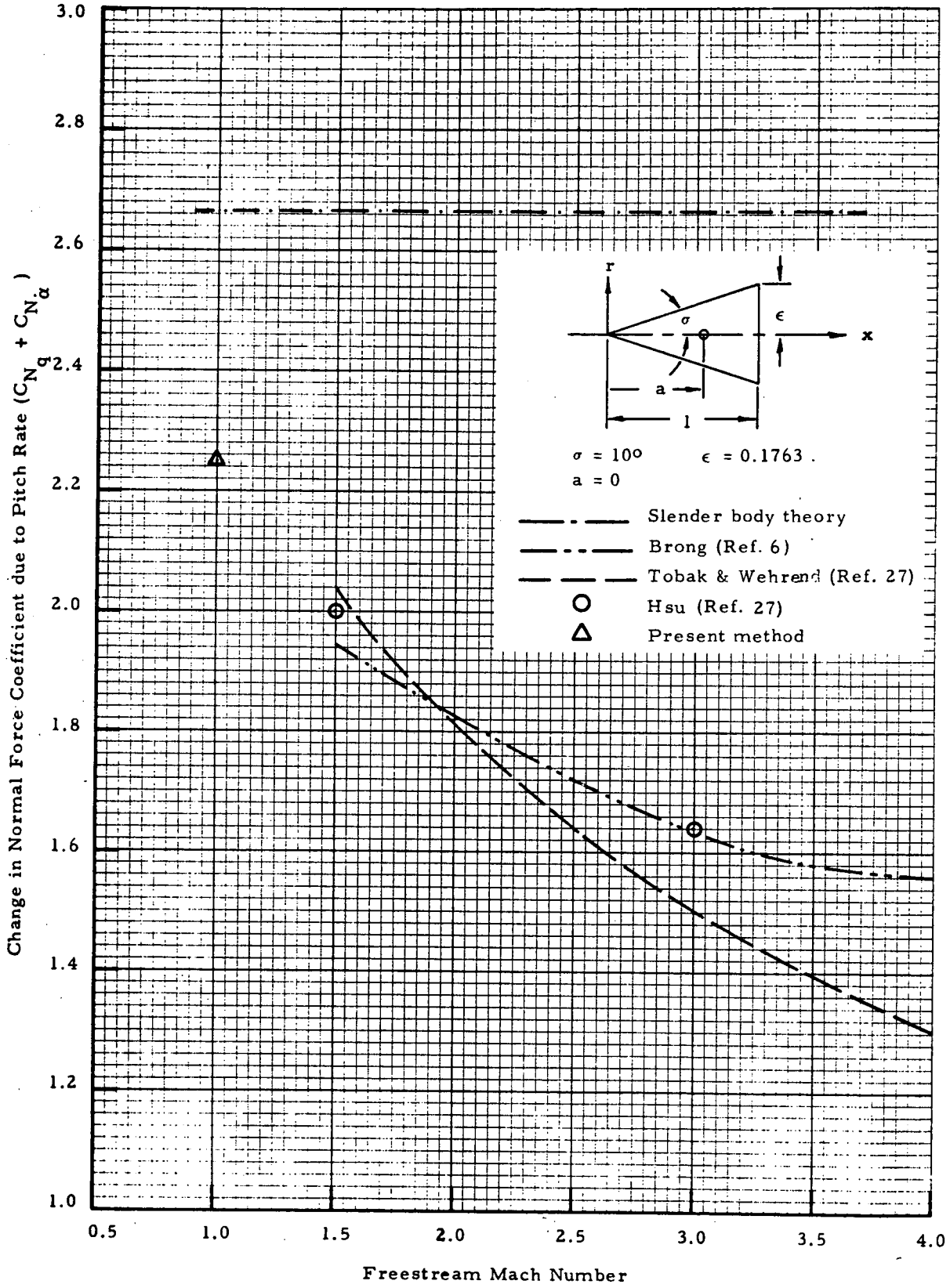

Fig. 9 - Effect of Mach Number on the Change in Normal Force Coefficient due to Pitch Rate for a 10-Degree Cone with Pitch Axis Location at a = 0.

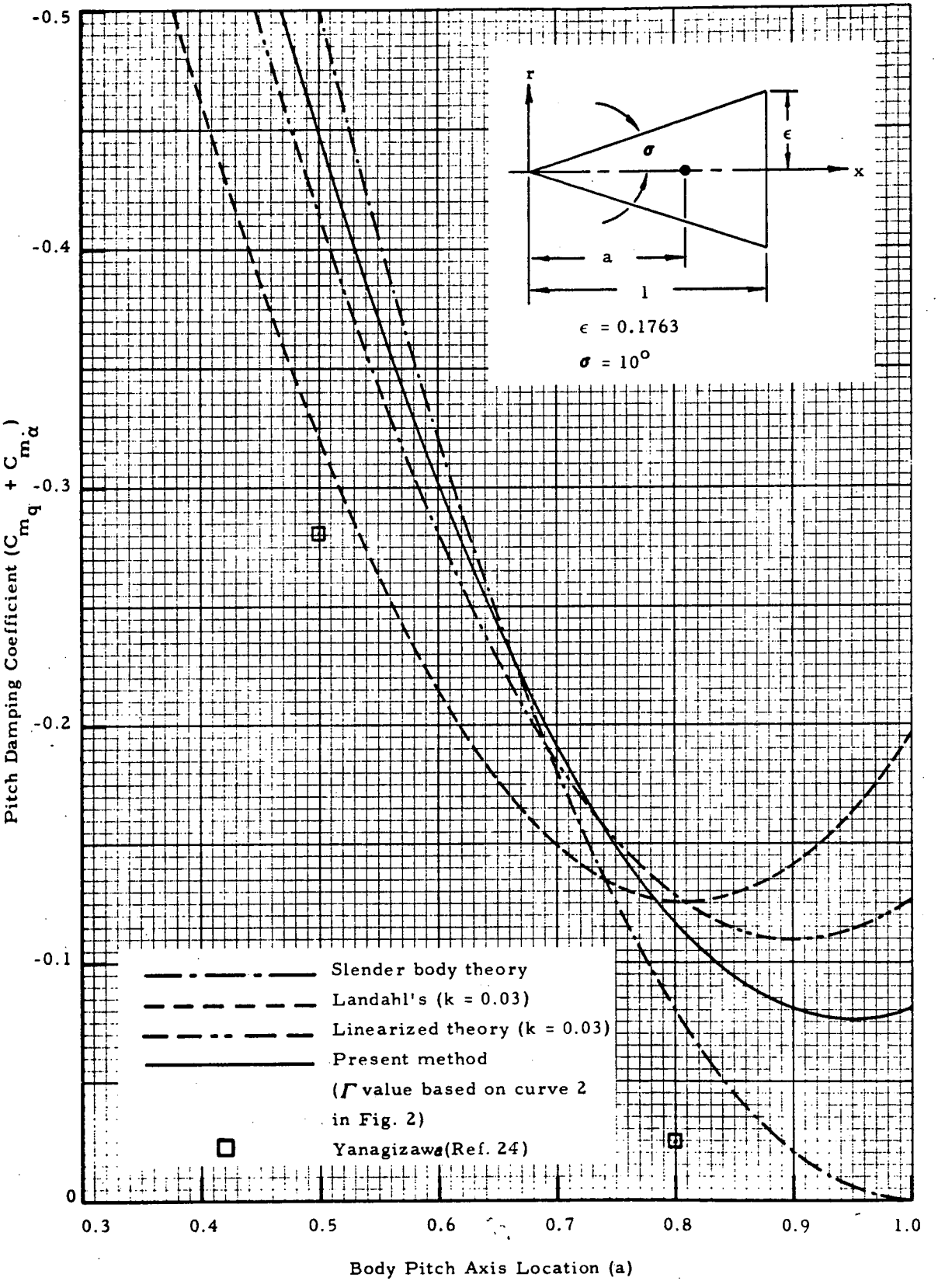

Fig. 10 - Damping-in-Pitch Moment Coefficient for a 10-Degree Cone at M_∞ = 1.0 vs Pitch Axis Location.

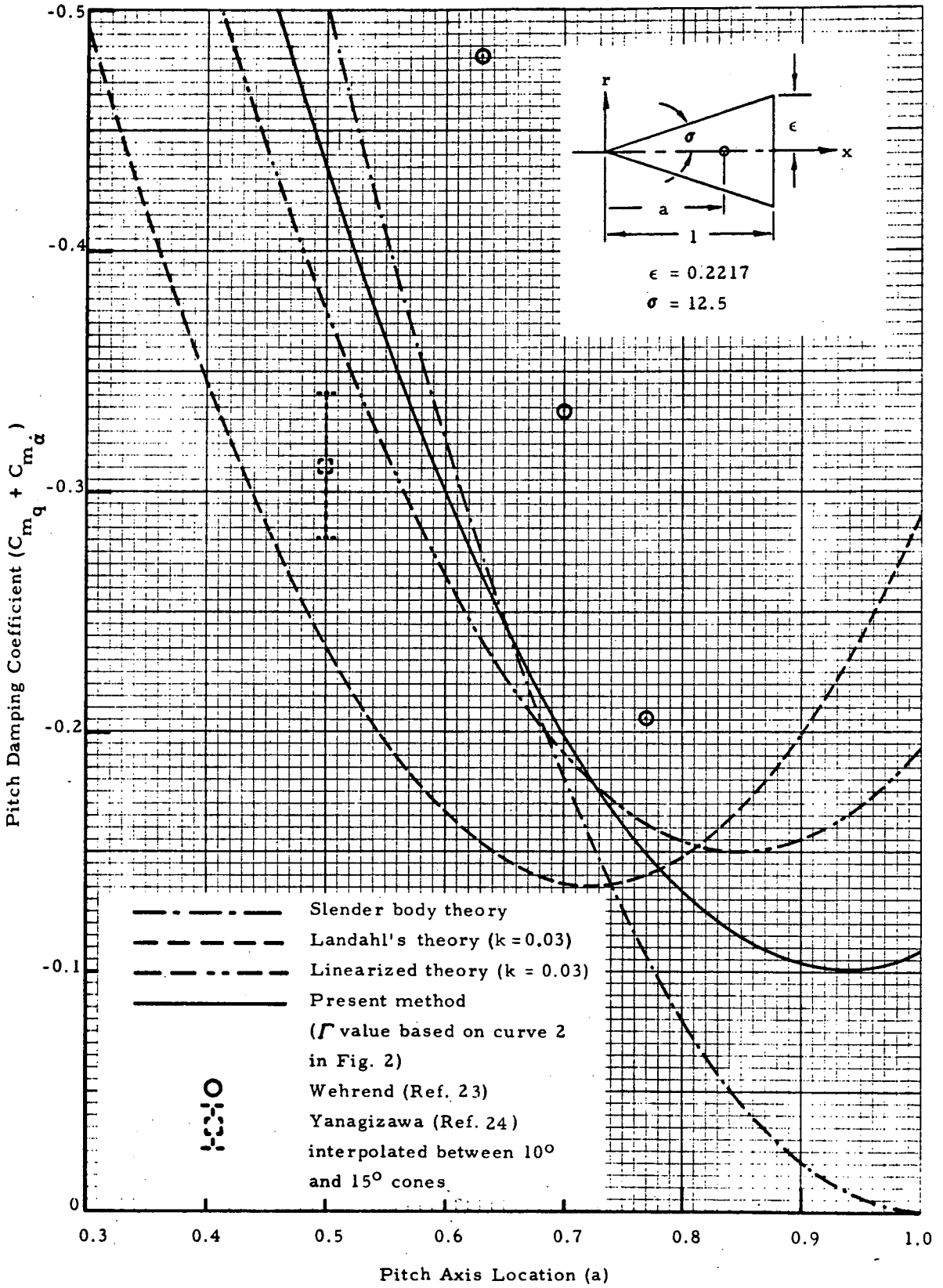

Fig. 11 - Damping-in-Pitch Moment Coefficient for a 12.5-Degree Cone at M_∞ = 1.0 vs Pitch Axis Location.

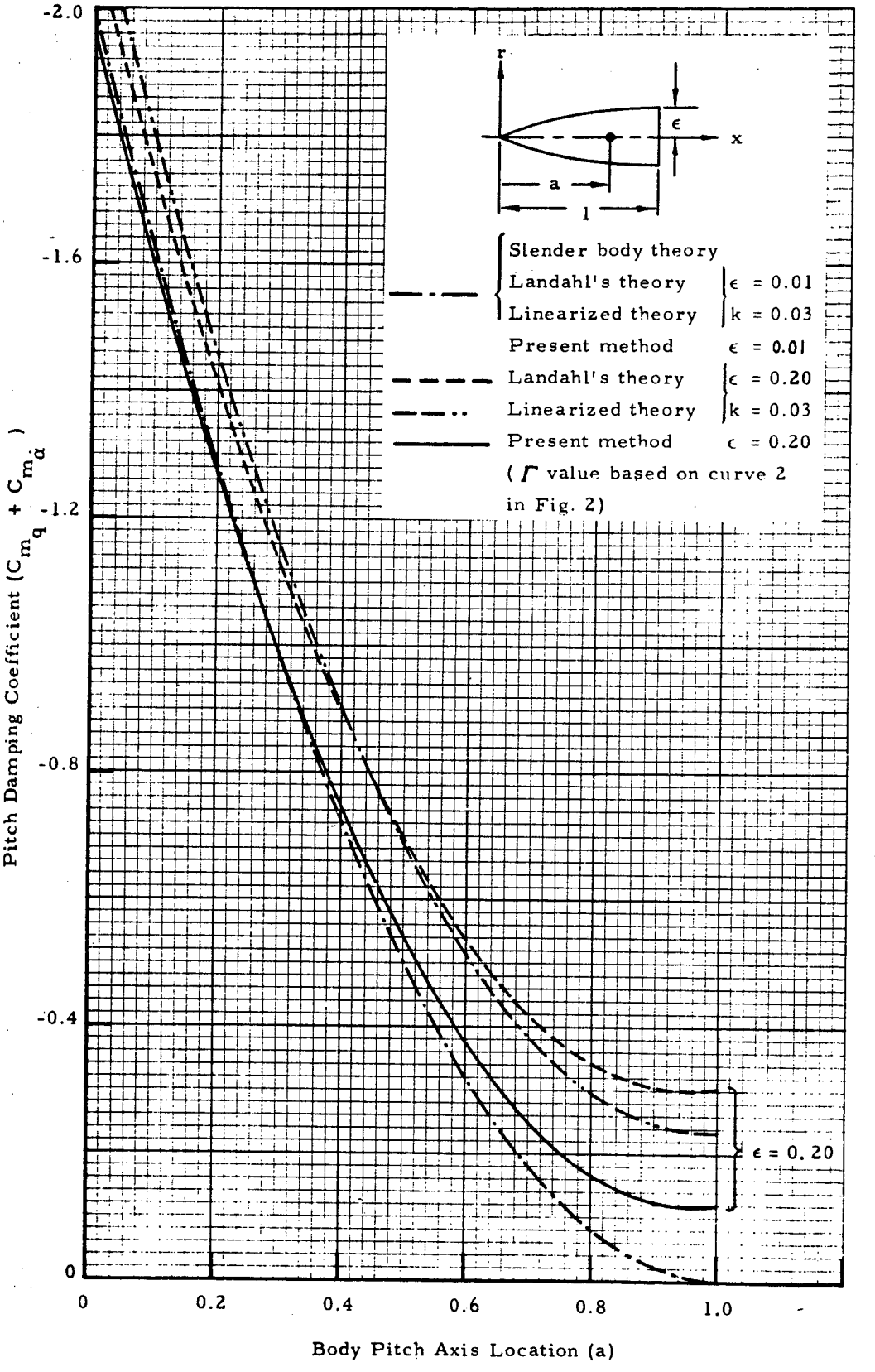

Fig. 12 - Damping-in-Pitch Moment Coefficient for Parabolic Ogives at M_∞ = 1.0 vs Pitch Axis Location.

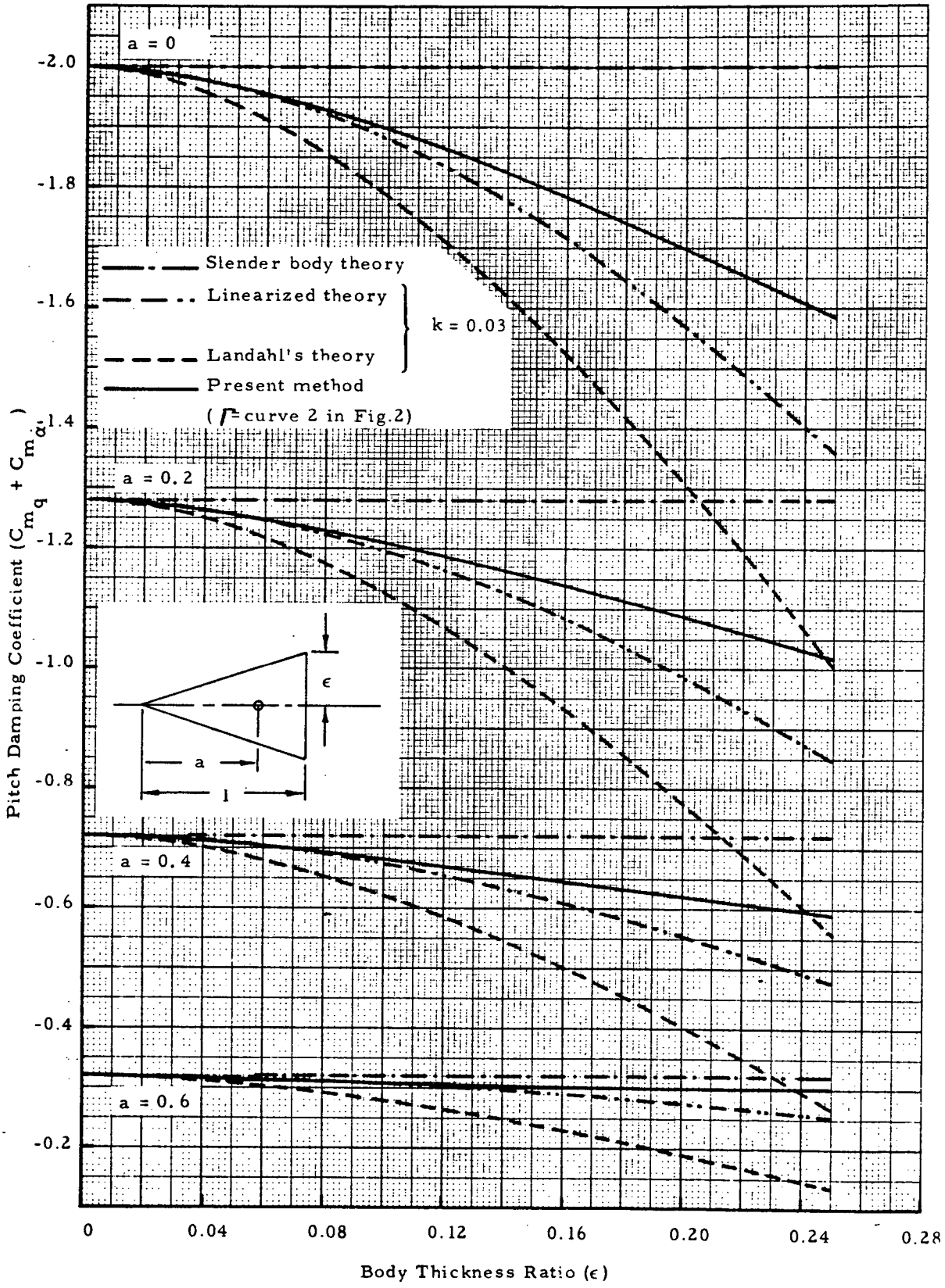

Fig. 13 - Effect of Thickness Ratio on Damping-in-Pitch Moment Coefficient for Cones at M_∞ = 1.0 with Various Pitch Axis Locations.

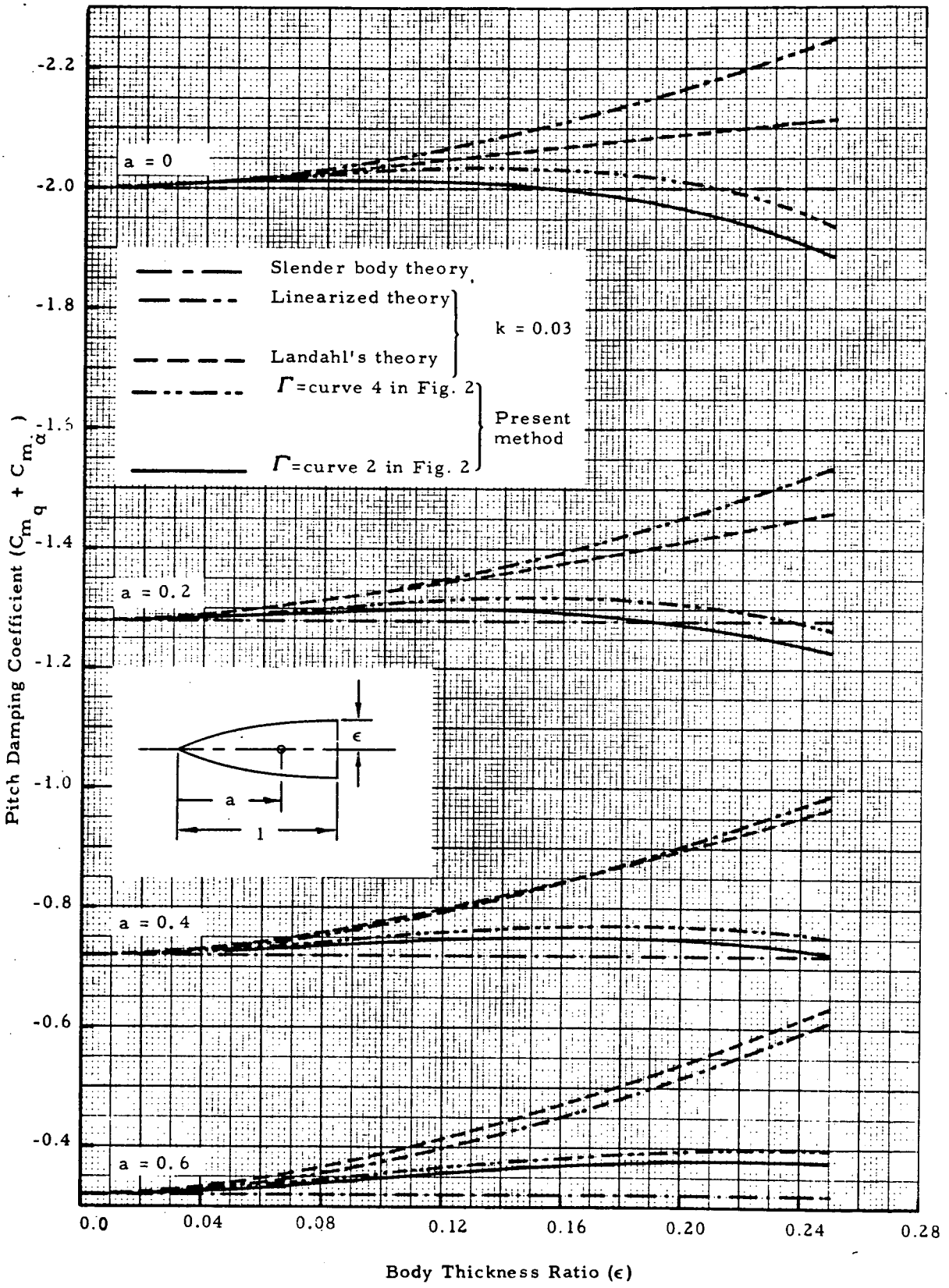

Fig. 14. - Effect of Thickness Ratio on Damping-in-Pitch Moment Coefficient for Parabolic Ogives at M_∞= 1.0 with Various Pitch Axis Locations.

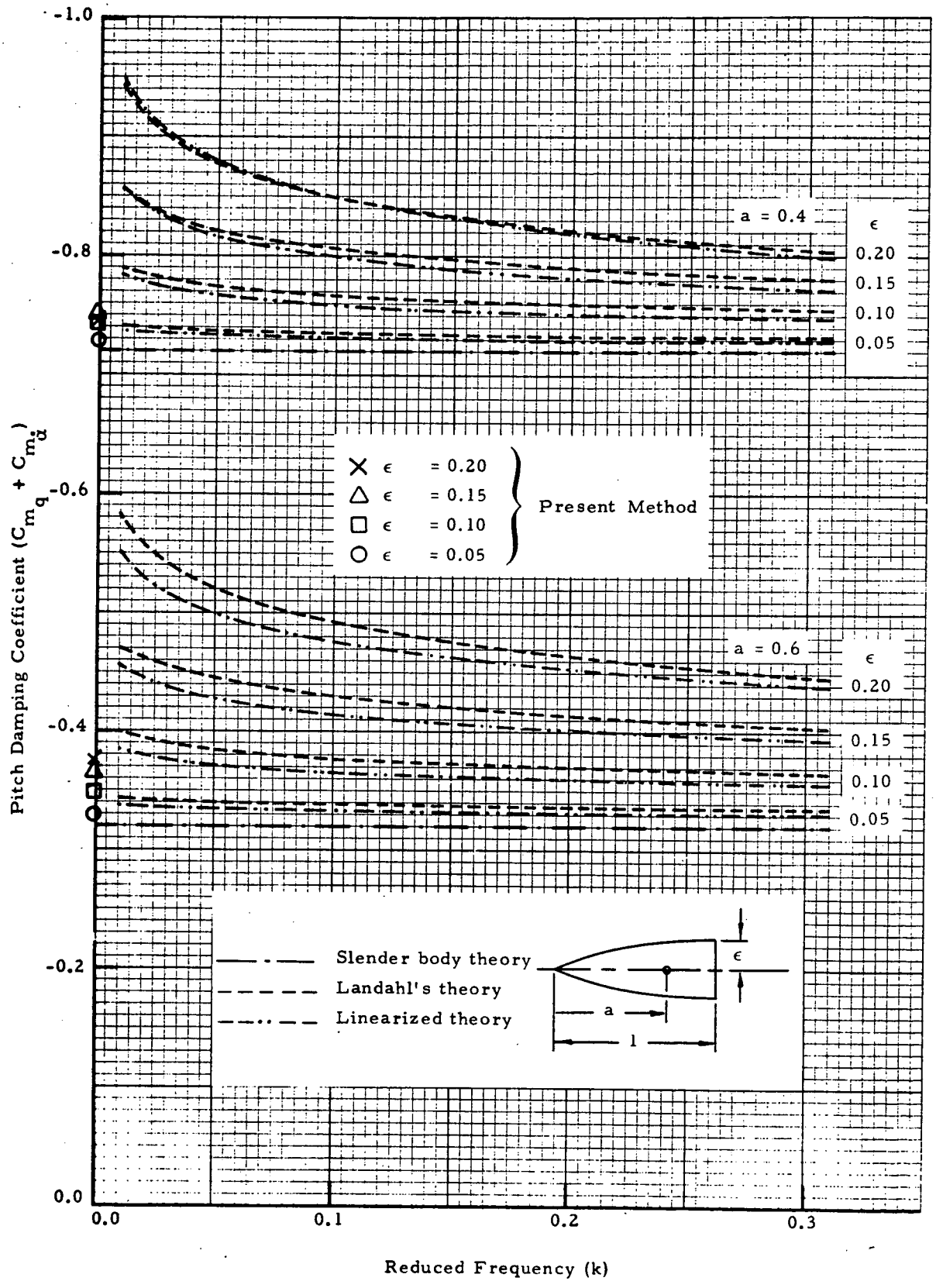

Fig. 15 - Damping-in-Pitch Moment Coefficient for Parabolic Ogives at M_∞ = 1.0 vs Reduced Frequency with Pitch Axis Locations at a 0.4 and 0.6.

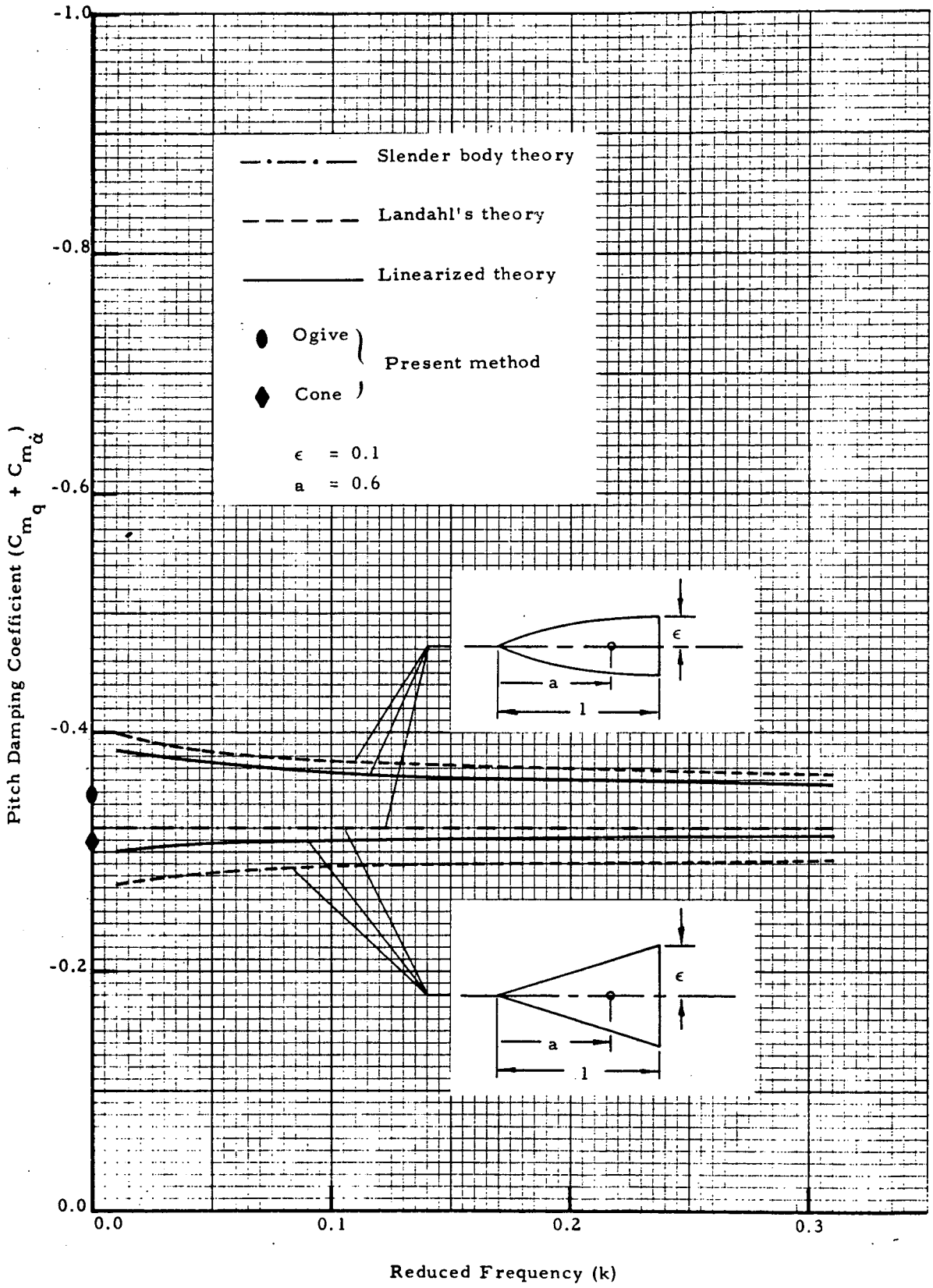

Fig. 16 - Damping-in-Pitch Moment Coefficient for a Cone and a Parabolic Ogive of the Same Thickness Ratio $\epsilon = 0.1$ at $M_\infty = 1.0$ versus Reduced Frequency with Pitch Axis Location at $a = 0.6$

Appendix A

SECOND ORDER DOUBLET DISTRIBUTION FUNCTION

Appendix A

The derivation of $F^{(2)}(x)$ is straightforward; however, it involves a lengthy step to arrive at the final result, Eq. (3.14). For the purpose of keeping record of the result obtained, the step-by-step derivation is presented in this appendix.

For convenience Eqs. (3.12), (3.13) and Eq. (2.18) are rewritten here:

$$F^{(1)}(x) = 2Q(x)\left[\delta + (x-a)\,\dot{\delta}\right] \tag{3.12}$$

$$F^{(2)}(x) = \left[-\frac{Q'^2(x)}{\pi}\right]\delta + \left[-(x-a)\frac{Q'^2(x)}{\pi}\right]\dot{\delta} + 2Q(x)\frac{\partial \zeta^{(1)}}{\partial r} \tag{3.13}$$

$$\zeta(x,r;\Gamma) = \frac{\Gamma r}{8\pi}\left[F'(x)\left(\ell n\frac{\Gamma r^2}{4} + c - 1\right) - \int_0^x F''(\xi)\,\ell n(x-\xi)\,d\xi\right]$$

$$+\frac{ikr}{4\pi}\left[F'(x)\left(\ell n\frac{\Gamma r^2}{4} + c\right) - \int_0^x F''(\xi)\,\ell n(x-\xi)\,d\xi\right]. \tag{2.18}$$

From Eq. (2.18) one may write

$$\zeta^{(1)}(x,r;\Gamma) = \frac{\Gamma r}{8\pi}\left[F'^{(1)}(x)\left(\ell n\frac{\Gamma r^2}{4} + c - 1\right) - \int_0^x F''^{(1)}(\xi)\,\ell n(x-\xi)\,d\xi\right]$$

$$+\frac{ikr}{4\pi}\left[F'^{(1)}(x)\left(\ell n\frac{\Gamma r^2}{4} + c\right) - \int_0^x F''^{(1)}(\xi)\,\ell n(x-\xi)\,d\xi\right], \tag{A.1}$$

then by making use of the relation in Eq. (3.12)

$$\zeta^{(1)}(x, r; \Gamma) = \frac{\Gamma r}{4\pi}\left\{\delta\, Q'(x) + \dot{\delta}\left[(x-a)\, Q'(x) + Q(x)\right]\right\}\left\{\ell n \frac{\Gamma r^2}{4} + c - 1\right\}$$

$$- \frac{\Gamma r}{4\pi}\int_0^x \left\{\delta\, Q''(x) + \dot{\delta}\left[(x-a)\, Q(x) + 2Q'(x)\right]\right\}\left\{\ell n(x-\xi)\right\} d\xi$$

$$+ \frac{i k r}{2\pi}\left\{\delta\, Q'(x) + \dot{\delta}\left[(x-a)\, Q'(x) + Q(x)\right]\right\}\left\{\ell n \frac{\Gamma r^2}{4} + c\right\}$$

$$- \frac{i k r}{2\pi}\int_0^x \left\{\delta\, Q''(x) + \dot{\delta}\left[(x-a)\, Q''(x) + 2Q'(x)\right]\right\}\left\{\ell n(x-\xi)\right\} d\xi$$

$$= \delta\left[\frac{\Gamma r}{4\pi}\left\{\left(\ell n \frac{\Gamma r^2}{4} + c - 1\right) Q'(x) - \int_0^x Q''(x) \cdot \ell n(x-\xi)\, d\xi\right\}\right.$$

$$- \frac{k^2 r}{2\pi}\left\{\left[(x-a)\, Q'(x) + Q(x)\right]\left[\ell n \frac{\Gamma r^2}{4} + c\right] - \int_0^x \left[(\xi - a)\, Q''(\xi)\right.\right.$$

$$\left.\left. + 2Q'(\xi)\right] \ell n(x-\xi)\, d\xi\right\}\Bigg]$$

$$+ \dot{\delta}\left[\frac{r}{2\pi}\left\{\left(\ell n \frac{\Gamma r^2}{4} + c\right) Q'(x) - \int_0^x Q''(x)\, \ell n(x-\xi)\, d\xi\right\}\right.$$

$$+ \frac{\Gamma r}{4\pi}\left\{\left[(x-a)\, Q'(x) + Q(x)\right]\left[\ell n \frac{\Gamma r^2}{4} + c - 1\right]\right.$$

$$- \int_0^x \left[(\xi - a)\, Q''(\xi) + 2 Q'(\xi) \right] \ell n(x - \xi)\, d\xi \Bigg\} \Bigg]$$

$$= \delta\, r \left[\frac{\Gamma}{4\pi}\, Q'(x)\, \ell n \frac{\Gamma r^2}{4} + \frac{\Gamma}{4\pi}\, (c - 1)\, Q'(x) - \frac{\Gamma}{4\pi} \int_0^x Q''(\xi)\, \ell n(x - \xi)\, d\xi \right] - O\left[k^2 \delta\right]$$

$$+ \dot{\delta}\, r \left[\frac{\Gamma}{4\pi} \left\{ \left[(x - a)\, Q'(x) + Q(x) \right] \ell n \frac{\Gamma r^2}{4} + \frac{\Gamma}{4\pi}\, (c - 1) \left[(x - a)\, Q'(x) + Q(x) \right] \right.\right.$$

$$\left.\left. - \int_0^x \left[(\xi - a)\, Q''(\xi) + 2 Q'(\xi) \right] \ell n(x - \xi)\, d\xi \right\} \right.$$

$$\left. + \frac{1}{2\pi} \left\{ Q'(x)\, \ell n \frac{\Gamma r^2}{4} + c\, Q'(x) - \int_0^x Q''(\xi)\, \ell n(x - \xi)\, d\xi \right\} \right]$$

$$\cong \delta\, r \left[\left\{ \ell n \frac{\Gamma r^2}{4} \right\} \left\{ \frac{\Gamma}{4\pi}\, Q'(x) \right\} + \frac{\Gamma}{4\pi} \left\{ (c - 1)\, Q'(x) - \int_0^x Q''(\xi)\, \ell n(x - \xi)\, d\xi \right\} \right]$$

$$+ \dot{\delta}\, r \left[\left\{ \frac{\Gamma}{4\pi} \left[(x - a)\, Q'(x) + Q(x) \right] + \frac{Q'(x)}{2\pi} \right\} \left\{ \ell n \frac{\Gamma r^2}{4} \right\} \right.$$

$$+ \frac{\Gamma}{4\pi} \left\{ (c - 1) \left[(x - a)\, Q'(x) + Q(x) \right] - \int_0^x \left[(\xi - a)\, Q''(\xi) + 2 Q'(\xi) \right] \ell n(x - \xi)\, d\xi \right\}$$

$$\left. + \frac{1}{2\pi} \left\{ c\, Q'(x) - \int_0^x Q''(\xi)\, \ell n(x - \xi)\, d\xi \right\} \right]$$

$$= \delta r \left[\left(\ell n \frac{\Gamma r^2}{4} \right) V_R + Y_R \right] + \dot{\delta} r \left[\left(\ell n \frac{\Gamma r^2}{4} \right) V_I + Y_I \right] \tag{A.2}$$

where

$$V_R = \frac{\Gamma}{4\pi} Q'(x) \tag{A.3}$$

$$Y_R = \frac{\Gamma}{4\pi} \left[(c-1) Q'(x) - \int_o^x Q''(\xi) \ell n(x-\xi) d\xi \right] \tag{A.4}$$

$$V_I = \frac{\Gamma}{4\pi} \left[(x-a) Q'(x) + Q(x) \right] + \frac{Q'(x)}{2\pi} \tag{A.5}$$

$$Y_I = \frac{\Gamma}{4\pi} \left\{ (c-1) \left[(x-a) Q'(x) + Q(x) \right] - \int_o^x \left[(\xi - a) Q''(\xi) + 2Q'(\xi) \right] \ell n(x-\xi) d\xi \right\}$$

$$+ \frac{1}{2\pi} \left\{ c\, Q'(x) - \int_o^x Q''(\xi) \ell n(x-\xi) d\xi \right\} . \tag{A.6}$$

Note that the terms containing $k^2 \delta$ were ignored for this particular case because k is considered to be small and use of the following relation

$$\delta = \delta_o e^{ikt} \qquad (\dot{\delta} = ik\delta)$$

has been made to eliminate i.

$$\therefore \quad \frac{\partial \zeta^{(1)}}{\partial r} = \delta \left[\left(\ell n \frac{\Gamma r^2}{4} \right) V_R + Y_R \right] + \delta r \left[\frac{2}{r} V_R \right]$$

$$+\dot{\delta}\left[\left(\ell n\frac{\Gamma r^2}{4}\right)V_I + Y_I\right] + \dot{\delta}\, r\left[\frac{2}{r}V_I\right]$$

$$= \delta\left[V_R\left(2 + \ell n\frac{\Gamma r^2}{4}\right) + Y_R\right] + \dot{\delta}\left[V_I\left(2 + \ell n\frac{\Gamma r^2}{4}\right) + Y_I\right]$$

$$= \delta\, Z_R + \dot{\delta}\, Z_I ,$$

where

$$Z_R = V_R\left(2 + \ell n\frac{\Gamma r^2}{4}\right) + Y_R \qquad \text{(A.7)}$$

$$Z_I = V_I\left(2 + \ell n\frac{\Gamma r^2}{4}\right) + Y_I \ . \qquad \text{(A.8)}$$

Finally, one obtains

$$F^{(2)}(x) = \delta\left[-\frac{Q'^2(x)}{\pi} + 2\, Z_R\, Q(x)\right] + \dot{\delta}\left[-(x-a)\frac{Q'^2(x)}{\pi} + 2\, Z_I\, Q(x)\right].$$

Appendix B

FURTHER SIMPLIFICATION OF PRESSURE COEFFICIENTS

Appendix B

In order to calculate C_{m_δ} and $C_{m_{\dot{\delta}}}$ in accordance with the assumption that the body is slender and terms smaller than order ϵ^2 can be neglected, the C_{p_1} and C_{p_2} in the second term on the right-hand side of Eqs. (4.11) and (4.13) need to be simplified further. The simplified C_{p_1} and C_{p_2}, by neglecting the higher order terms than ϵ, are respectively denoted by C_{p_3} and C_{p_4}.

For convenience Eq. (4.2) is repeated here and the order of each term in ϵ is noted directly below each term.

$$C_{p_1} = \underset{\epsilon}{-2\,\Psi_x^{(1)+(2)}} \underset{\epsilon^2 \cdot \epsilon}{- R'^2(x) \cdot \Psi_x^{(1)}} \tag{B.1}$$

$$C_{p_2} = \underset{\epsilon}{-2\,(\lambda_x + \Psi)^{(1)+(2)}} \underset{\epsilon}{+2} \underset{(\epsilon+\epsilon)\cdot\epsilon^2}{\left[\Psi^{(1)} + R(x)\right]\phi_x^{(1)}} \underset{\epsilon^2\cdot(\epsilon-\epsilon-\epsilon)}{- R'^2(x)\left[\lambda_x^{(1)} - \Psi^{(1)} - 2R(x)\right]} \tag{B.2}$$

It is obvious that only the first term on the right-hand side of Eqs. (B.1) and (B.2) needs further consideration. The expressions for Ψ, Ψ_x and λ_x are:

$$\Psi^{(1)+(2)} = \frac{Q}{\pi R}(1+Y_R) - \frac{Q'^2}{2\pi^2 R} + V_R \qquad \text{(B.3)}$$

$$\underbrace{\epsilon \cdot (\epsilon^0 + \epsilon^2)}_{\epsilon^3} \qquad \epsilon^3 \qquad \epsilon^3$$

$$\Psi_x^{(1)+(2)} = \frac{Q'}{\pi R}(1+Y_R) + \frac{Q}{\pi R}(Y_R)_x - \frac{Q'Q''}{\pi^2 R} + (V_R)_x \qquad \text{(B.4)}$$

$$\underbrace{\epsilon \cdot (\epsilon^0 + \epsilon^2)}_{\epsilon^3} \quad \epsilon \cdot \epsilon^2 \quad \epsilon^3 \quad \epsilon^3 \quad \epsilon^3 \quad \epsilon^3$$

$$\lambda_x^{(1)+(2)} = \frac{Q'}{\pi R}\left[(x-a) + Y_I\right] + \frac{Q}{\pi R}\left[1 + (Y_I)_x\right] - \frac{Q'Q''}{\pi^2 R}(x-a) - \frac{Q'^2}{2\pi^2 R} + (V_I)_x . \qquad \text{(B.5)}$$

$$\epsilon \cdot (\epsilon^0 + \epsilon^2) \quad \epsilon \cdot (\epsilon^0 + \epsilon^2) \quad \epsilon^3 \cdot \epsilon^0 \quad \epsilon^3 \quad \epsilon^3$$

By retaining the terms containing ϵ in Eqs. (B.3), (B.4) and (B.5), one finally obtains the expressions for C_{p_3} and C_{p_4} as follows:

$$C_{p_3} = -2\frac{Q'}{\pi R}$$

$$C_{p_4} = -2\left[\frac{Q'}{\pi R}(x-a) + 2\frac{Q}{\pi R}\right],$$

which can be written as

$$C_{p_3} = -2\,\Psi_x^{(1)} \qquad \text{(B.6)}$$

$$C_{p_4} = -2\left(\lambda_x^{(1)} + \Psi^{(1)}\right). \qquad \text{(B.7)}$$

Appendix C
INTEGRAL TERMS

Appendix C

To simplify the writing in the text some of the integration terms are defined in this appendix as follows:

$$\left.\begin{aligned} I_1 &= \int_0^x Q'(\xi)\, \ell n(x-\xi)\, d\xi \\ I_2 &= \int_0^x Q''(\xi)\, \ell n(x-\xi)\, d\xi \\ I_3 &= \int_0^x \xi\, Q''(\xi)\, \ell n(x-\xi)\, d\xi \\ I_4 &= \int_0^x Q'''(\xi)\, \ell n(x-\xi)\, d\xi \\ I_5 &= \int_0^x \xi\, Q'''(\xi)\, \ell n(x-\xi)\, d\xi \end{aligned}\right\} \qquad (C.1)$$

If the radius of the body under consideration is written in the following form

$$R(x) = \epsilon Z(x) = \epsilon(Ax + Bx^2),$$

then Eqs. (C.1) become

$$\left.\begin{aligned} I_1 &= \pi\epsilon^2\left[\quad 2A^2 \cdot J_2 + 6AB \cdot J_3 + 4B^2 \cdot J_4\right] \\ I_2 &= \pi\epsilon^2\left[2A^2 \cdot J_1 + 12AB \cdot J_2 + 12B^2 \cdot J_3\right] \\ I_3 &= \pi\epsilon^2\left[\quad 2A^2 \cdot J_2 + 12AB \cdot J_3 + 12B^2 \cdot J_4\right] \\ I_4 &= \pi\epsilon^2\left[12AB \cdot J_1 + 24B^2 \cdot J_2\right] \\ I_5 &= \pi\epsilon^2\left[\quad 12AB \cdot J_2 + 24B^2 \cdot J_3\right] \end{aligned}\right\} \qquad (C.2)$$

where

$$J_n = \int_o^x \xi^{(n-1)} \ln(x-\xi)\, d\xi = \left[- \sum_{j=0}^{(n-1)} \frac{1}{(j+1)} + \ln x \right] \frac{x^n}{n}, \quad n = 1, 2, 3, 4$$